Distribution of glycinergic neurons in the brain of glycine transporter-2 Tg(glyt2:gfp) transgenic adult zebrafish

Please cite as: Barreiro-Iglesias, Anton; Mysiak, Karolina Sandra; Adrio, Fatima; Celina Rodicio, Maria; Becker, Catherina G.; Becker, Thomas; Anadon, Ramon / Distribution of glycinergic neurons in the brain of glycine transporter-2 Tg(glyt2:gfp) transgenic adult zebrafish : Relation with brain-spinal descending systems. In: Journal of Comparative Neurology, Vol. 521, No. 2, 01.02.2013, p. 389-425.
DOI: 10.1002/cne.23179

Distribution of Glycinergic Neurons in the Brain of Glycine Transporter-2 Tg(*glyt2:gfp*) Transgenic Adult Zebrafish: Relation with Brain-Spinal Descending Systems

Antón Barreiro-Iglesias[1,2], Karolina Sandra Mysiak[2], Fátima Adrio[1], María Celina Rodicio[1], Catherina G. Becker[2], Thomas Becker[2], and Ramón Anadón[1]

[1]Department of Cell Biology and Ecology, CIBUS, Faculty of Biology, University of Santiago de Compostela, 15782 Santiago de Compostela, Spain

[2]Centre for Neuroregeneration, School of Biomedical Sciences, University of Edinburgh, The Chancellor's Building, 49 Little France Crescent, Edinburgh EH16 4SB, United Kingdom

The glycine transporter GLYT2 in the brain of adult zebrafish

With 59 Text Pages, and 19 Figures

Key words: glycinergic system, reticular formation, octavolateral area, Mauthner neuron, GFP transgenic, glycine transporter 2, glycine immunohistochemistry, in situ hybridization, pineal, *Danio rerio*, Teleosts

Corresponding author: Ramón Anadón
E-mail: ramon.anadon@usc.es

Acknowledgements. We thank Dr. Joseph R. Fetcho his generous permission of using the GLYT2 zebrafish transgenic line for the present investigation. This work was supported by grants from the Xunta de Galicia

(INCITE08PXIB200063PR) and the Spanish Ministry of Science and Innovation (BFU2007-61056/BFI and BFU2010-17174/BFI) to M.C. Rodicio, a grant from the Xunta de Galicia (INCITE09ENA200036ES) to R. Anadón and grants from the BBSRC, and a joint grant from the Packard Center for ALS Research at Johns Hopkins and the Euan MacDonald Centre for Motor Neurone Disease Research at the University of Edinburgh to C.G. Becker and T. Becker.

Conflict of interest statement. All authors declare no conflict of interest.

Role of authors. All authors had access to all the data in the study and take responsibility for the integrity of the data and the accuracy of the data analysis. Study concept and design: AB-I, RA, CGB, TB. Acquisition of data: AB-I, KSM, FA, TB. Analysis and interpretation of data: RA, AB-I, KSM, FA, TB. Drafting of the manuscript: RA, AB-I, KSM, FA, TB. Critical revision of the manuscript for important intellectual content: MCR, CGB, TB, RA. Obtained funding: MCR, CGB, TB.

ABSTRACT

We used a Tg(*glyt2:gfp*) transgenic zebrafish expressing the green fluorescent protein (GFP) under control of the glycine transporter 2 (GLYT2) regulatory sequences to study for the first time the glycinergic neurons in the brain of an adult teleost. We also performed *in situ* hybridization using a GLYT2 probe and glycine immunohistochemistry. This study was combined with biocytin tract tracing from the spinal cord to reveal descending glycinergic pathways. A few groups of GFP-positive/GLYT2 negative cells were observed in the midbrain and forebrain, including numerous pinealocytes. Conversely, a small nucleus of the midbrain tegmentum, was GLYT2 positive but GFP negative. Most of the GFP-positive and GLYT2-positive neurons were observed in the rhombencephalon and spinal cord, and a proportion of these cells showed double GLYT2/GFP labeling. In the hindbrain, GFP/GLYT2-positive populations were observed in the medial octavolateral nucleus, the secondary, magnocellular and descending octaval nuclei, the viscerosensory lobes and reticular populations distributed from trigeminal to vagal levels. No glycinergic

cells were observed in the cerebellum. Tract tracing revealed three conspicuous pairs of GFP/GLYT2-positive reticular neurons projecting to the spinal cord. In the spinal cord, GFP/GLYT2-positive cells were observed in the dorsal and ventral horns. GFP-positive fibers were observed from the olfactory bulbs to the spinal cord, although its density varied among regions. The Mauthner neurons received very rich GFP-positive innervation, mainly around the axon cap. Comparison of the zebrafish glycinergic system with those of other adult vertebrates reveals shared patterns but also divergent traits in the evolution of this system.

INTRODUCTION

The amino acid glycine is one of the two fast inhibitory neurotransmitters used by neurons in the central nervous system of vertebrates. Early evidence that glycine might act as a neurotransmitter in the cat spinal cord was provided by Aprison and Werman (1965), and since then the function of glycine in the spinal cord and brain has received much attention (see Bowery and Smart, 2006). Inhibitory action of glycine is mediated by its action on glycine receptors in postsynaptic membranes. Antagonists of glycine receptors (such as strychnine) have been long time used to characterize the glycinergic synapses (Curtis et al., 1968; Young and Snyder, 1974; Aprison and Daly, 1978). The glycine receptors are ligand-gated chloride channels whose fast opening by glycine leads generally to neuron membrane hyperpolarization (Young and Snyder, 1974). Action of glycine at glycinergic synapses ceases by removing the neurotransmitter from the synaptic cleft by glycine transporters (Liu et al., 1992, 1993; Guastella et al., 1992; Smith et al., 1992). Transport by the glycine transporters 1 and 2 (GLYT1 and GLYT2) is mainly mediated by glia and neurons, respectively (Zafra et al., 1995a,b; Poyatos et al., 1997; Aragón and López-Corcuera, 2003). Glycine is also a coagonist of NMDA-type glutamate receptors (Johnson and Ascher, 1987; Parsons et al., 1998), being thus probably involved in complex neural processes.

The introduction of antibodies raised against glycine-protein conjugates allowed the study of putative glycinergic neurons and/or fibers in various regions of the CNS of mammals (Campistron et al., 1986; Wenthold et al.,

1987; Van den Pol and Gorcs, 1988; Saint Marie et al., 1989; Walberg et al., 1990; Pourcho et al., 1992; Rampon et al., 1996). Studies of distribution of glycinergic neurons in the adult brain of non-mammalian vertebrates using these methods are scant. Early studies of glycinergic neurons with these methods in non-mammalian vertebrates have been done in embryonic animals (Dale et al., 1986; Roberts et al., 1988). A major shortcoming of these immunohistochemical methods is that in general the amounts of glycine in cell perikarya are low and are hardly to be demonstrated in adults. In some instances, as in amphibians (Reichenberger et al., 1993, 1997; Landwehr and Dicke, 2005), lamprey (Villar-Cerviño et al., 2008a,b, 2009) and sturgeon (Adrio et al., 2011), glycine antibodies yielded good perikarya staining.

The cloning of glycine transporters 1 and 2 (GLYT1 and GLYT2) led to the production of specific antibodies against these transporters (Zafra et al., 1995a,b), and the demonstration that GLYT2 is mostly expressed in glycinergic neurons (Poyatos et al., 1997). This allowed using GLYT2 *in situ* hybridization and immunohistochemistry to reveal the glycinergic populations in rodent brains (rat: Zafra et al., 1995a,b; Poyatos et al., 1997; Aragón and López-Corcuera, 2003; Tanaka et al., 2003; Tanaka and Ezure, 2004), being a useful alternative to the use of glycine antibodies. Again, the use of GLYT2 antibodies in mammalian brain was much more effective to reveal terminals than neuronal perikarya. The use of transgenic mice expressing a fluorescent protein gene under control of GLYT2 regulatory sequences allowed labeling all parts of glycinergic neurons (perikarya, dendrites and axons) in an unprecedented level of detail (Zeilhofer et al., 2005).

Although the brain of teleosts has been extensively investigated with immunohistochemical methods for a number of neurotransmitters and neuropeptides, to the best of our knowledge no comprehensive study of the glycinergic populations in the brain of any adult teleost has been done. This is in striking contrast to the fact that the glycinergic synapses on Mauthner cells in teleosts have received notable attention, including immunohistochemical studies with antibodies against glycine or the glycine receptor (Seitanidou et al., 1988; Triller et al., 1993, 1997; Legendre and Korn, 1994). *In situ* hybridization has also revealed the wide distribution of mRNA of glycine receptor subunits in the adult zebrafish brain (Imboden et al., 2001). A single

study of the spinal cord in adult carp has described the glycinergic neurons using glycine immunohistochemistry (Uematsu et al., 1993). In recent times, cloning of zebrafish GLYT1 and GLYT2 genes followed by *in situ* hybridization (Higashijima et al., 2004a,b,c) and obtaining of zebrafish green fluorescent protein(GFP)-GLYT2 transgenes [Tg(*glyt2:gfp*)] using BAC chromosomes (McLean et al., 2007) allowed to study glycinergic neurons in the brain and spinal cord of developing zebrafish. Specifically, the Tg(*glyt2:gfp*) transgene allowed to study the morphology and physiology of inhibitory neurons in larval zebrafish and to characterize individual GFP-expressing cells as glycinergic (McLean et al., 2007; Liao and Fetcho, 2008; Kinkhabwala et al., 2011; Koyama et al., 2011; Moly and Hatta, 2011).

The aim of this work was to investigate the organization of glycinergic neurons and fibers in the adult brain of a model vertebrate, the zebrafish *Danio rerio*, by using a well characterized Tg(*glyt2:gfp*) transgenic line employed in studies of the glycinergic system in embryos and early larvae. This approach allows also combination with retrograde neuronal tracers in order to better decipher the relationship between the glycinergic and the well-characterized brain-spinal projection systems.

MATERIAL AND METHODS

Animals

Twelve Tg(*glyt2:gfp*) transgenic adult zebrafish (*Danio rerio*, Cyprinidae) of both sexes were used in the present study. All transgenic fish were kept and bred in our laboratory fish facility according to standard methods (Westerfield, 1989). Three additional wild-type zebrafish were used for glycine immunohistochemistry. They were purchased in a pet-shop and used immediately. All experiments have been approved by the British Home Office and were performed according to European Union (86/609/EEC) and Spanish (Royal Decree 223/1998) regulations for the care and handling of animals in research. All experiments involving animals were conducted under deep anesthesia by immersion in 0.033% aminobenzoic acid ethylmethylester (MS222, Sigma; St. Louis MO) in phosphate buffered saline (PBS) for 10 minutes.

The glycine transporter-2 transgenic line

A transgenic fish was generated using a bacterial artificial chromosome DNA construct in which GFP was placed under the control of the *glycine transporter-2 cis*-regulatory elements and was used to generate stable transgenic lines by McLean et al. (2007), following the procedure detailed previously by Higashijima et al. (2004c). Several studies in larval zebrafish using these lines have reported consistent GFP expression in well-characterized glycinergic cells (Liao and Fetcho, 2008; Kinkhabwala et al., 2011; Koyama et al., 2011; Moly and Hatta, 2011).

Glycine transporter 2 in situ hybridization combined with GFP immunofluorescence

In order to assess if glycine transporter 2 is expressed by GFP-positive cells, we used GLYT2 *in situ* hybridization combined with GFP immunofluorescence in Tg(*glyt2:gfp*) transgenic adult zebrafish (n= 2). The method for *in situ* hybridization in combination with fluorescence has been described (Lieberoth et al., 2003). Briefly, for glyt2 *in situ* hybridization, Tg*(glyt2:gfp)* (McLean et al., 2007) fish were terminally anaesthetised by immersion in 0.1% MS222 in PBS and perfused with 4% paraformaldehyde. They were post-fixed in the same fixative for 2 days at 4ºC. The brains were dissected and embedded in 4% agar in PBS for vibratome sectioning. Transverse sections (50 µm in thickness) were transferred to PBS and stored at 4ºC overnight. The sections were hybridized with a digoxygenin (DIG) labeled GLYT2 probe (1:1000) at 65ºC overnight. The *GLYT2* fragment (1.7 kb in length) was obtained by using embryonic cDNA as a template (Higashijima et al., 2004a). The plasmid to generate the probe has been described in Higashijima et al. (2004a). Complementary RNA probes were tagged with digoxigenin (DIG). Alkaline phosphatase conjugated sheep anti-DIG antibody (Roche, Mannheim, Germany, Cat. No. 11 093 274 910; dilution 1:10 000) was added to the sections for overnight incubation at 4ºC. The colour signal was developed using nitro-blue tetrazolium (NTB) and 5-bromo-4-chloro-3'-indolyphosphate (BCIP) staining solution (Roche) for 2h or overnight at room temperature.

After removing the staining solution, the sections were incubated with chicken anti-GFP antibody (Abcam, Cambridge, UK, code Ab13970; dilution

1:500) for 2 days at 4ºC. The sections were incubated with Dylight-488 donkey anti-chicken secondary antibody (Stratech Scientific Ltd, Suffolk, UK, code 703-485-155; dilution 1:200) at room temperature for 1h, washed and mounted on SuperFrost 00® Plus slides in 70% glycerol in PBS. In the transgenic zebrafish brain, this anti-GFP antibody produced the same pattern of stained cells and fibers as shown by GFP fluorescence but often fluorescence intensity was more intense. Moreover, according to supplier data, the anti-GFP antibody does not stain any native protein band in western blots of rat brain lysates used for control. This antibody did not stain any brain structure in wild type zebrafish (Hunter et al., 2011; Kuscha et al., 2012).

Retrograde axonal tracing in transgenic zebrafish

Retrograde axonal tracing was performed in 5 adult Tg(*glyt2:gfp*) zebrafish from a spinal level 3.5 mm caudal to the obex (brainstem-spinal transition) under 0.033% MS222 anesthesia following the procedure described in Becker et al. (1997). The spinal cord was completely transected using Castroviejo scissors by accessing to it from one of the lateral sides of the animal. The neuronal tracer used was biocytin (Sigma). Biocytin was dissolved in distilled water to approximately 1 mg/10 µl. A small piece of gelatin foam (gel foam, Upjohn, Kalamazoo, MI) was saturated with the liquid and applied under the microscope between the cut ends of the transected spinal cord using a pair of fine forceps. The wound was sealed with histoacryl. Biocytin was allowed to be transported for 24 hours at room temperature.

Tissue preparation

Both traced (n=5) and control (n=5) Tg(*glyt2:gfp*) fish were deeply anaesthetized by immersion in 0.1% MS222 for 10 minutes and were perfused transcardially, first with 2 ml phosphate buffered saline (PBS; pH= 7.4) and then with 3 ml 4% paraformaldehyde in PBS. Fish were immersed in 4% paraformaldehyde at 4°C for a week. Then, the brain and rostral spinal cord were dissected out and rinsed in PBS, cryoprotected by overnight immersion in 30% sucrose in phosphate buffer, and then embedded in Tissue Tek (Sakura), frozen and cut in sagittal or transverse planes on a cryostat (25-30 µm thick). The cryostat sections were mounted on glass slides.

Indirect detection of biocytin

The presence of biocytin in cells and fibers was revealed by using streptavidin coupled to Dylight®549 (Vector Laboratories, Burlingame, CA; diluted 1:1000) in PBS with 0.3% Triton X-100, applied to sections of traced fish for 4 hours. After staining, sections were rinsed in PBS, then in distilled water and coverslipped with anti-fading mounting medium for fluorescence (Vectashield; Vector, Burlingame, CA).

Glycine immunofluorescence

In order to assess if glycine is accumulated in perikarya of putative glycinergic populations, we used glycine immunofluorescence following the procedure used by Villar-Cerviño et al. (2008a,b, 2009). For glycine immunofluorescence, three wild-type adult zebrafish were killed by immersion in 0.5% MS222 in water, and brains dissected out and fixed by immersion in cold 5% glutaraldehyde and 1% sodium metabisulfite in 0.05 M Tris-buffered saline (TBS; pH 7.4) for 15 hours. After fixation the brains were cryoprotected with 30% sucrose in 0.1 M phosphate buffer at pH 7.4 (PB), then embedded in Tissue Tek (Sakura, Torrance, CA), and frozen in liquid nitrogen-cooled isopentane. Serial transverse sections (16 µm thick) were cut on a cryostat and mounted on Superfrost Plus glass slides (Menzel, Braunschweig, Germany). Sections were pretreated with 0.2% $NaBH_4$ in deionized water for 45 minutes at room temperature to quench autofluorescence and incubated overnight at room temperature with rabbit polyclonal anti-glycine antibody (Immunosolution, Jesmond, Australia; code IG1003, batch 1953, dilution 1:3,000) in 0.05 M TBS (pH 7.4) with 1% sodium metabisulfite, 0.2% Triton X-100, and 15% normal goat serum. The sections were rinsed in TBS with 1% sodium metabisulfite, then incubated for 1 hour with Cy3-conjugated goat anti-rabbit immunoglobulin (Chemicon, dilution 1:200) and mounted with Vectashield. The secondary antibody was diluted in TBS containing 0.2% Triton X-100 and 3% normal goat serum.

The polyclonal rabbit anti-glycine antibody (Immunosolution) was raised against a glycine-porcine thyroglobin conjugate and tested by the supplier in sections of retina and cerebellum from various mammals and other vertebrates. It was also tested in dot-blot immunoassays with a variety of other amino acid conjugates, including the standard 20 amino acids found in

proteins; the nonprotein amino acids D-serine, D-alanine, and D-aspartate; GABA; and the glycine-containing tripeptide glutathione (GSH), which did not yield significant immunoreaction. The antibody was further tested in our laboratory by western blotting with fish (lamprey and sturgeon) brain protein extracts (Villar-Cerviño et al., 2008a,b, 2009; Adrio et al., 2011). In these blots, the antibody did not recognized any native protein band.

Photomicrographs and image presentation

Fluorescent and colorimetric signal of *in situ* hybridized brain sections were observed with an ApoTome (Zeiss, Jena, Germany) and a TCS-SP5 spectral laser confocal microscope (Leica, Wetzlar, Germany). Some pictures taken with an ApoTome were superimposed in false colour (GLYT2) using Photoshop® 7.0 (Adobe, San Jose, CA) and ImageJ (NIH, USA) software. For comparing the GLYT2 *in situ* reaction product and the GFP immunofluorescence in the same thin optical planes, we used a spectral confocal microscope with excitation wavelength lines of 647nm and 488nm, respectively, because at the 647nm the dark blue NTB-BCIP reaction product was fluorescent. Confocal photomicrographs of green GFP fluorescence in non-treated sections and double fluorescence in sections of biocytin transport experiments in transgenic fish were taken with the confocal microscope using excitation wavelength lines at 488 and 556 nm. For confocal photomicrographs of glycine immunohistochemistry in sections of wild-type zebrafish, we used a 556 nm excitation wavelength line. For presentation, some fluorescence photomicrographs were inverted and converted to gray scale; photomicrographs were adjusted for brightness and contrast with Photoshop CS (Adobe). Figures and lettering were composed using Photoshop CS. Schematic drawings were made with Corel Draw 12 (Corel, Ottawa, Canada).

Cell measurements

Cell diameters in sections of adult brain were measured with the aid of LAS AF Lite (Leica confocal software). The minor cell axis and the means ± standard deviations (S.D.) are provided.

Additional material

Series of Nissl-stained transverse sections of adult zebrafish brain from our collection were used for topographical purposes. Nissl-stained sections

were photographed with an Olympus photomicroscope (Tokyo, Japan) equipped with a color digital camera.

Nomenclature

The nomenclature used for the different nuclei of the zebrafish brain is based on those of Wullimann et al. (1996) and Castro et al. (2006a,b), unless explicitly adverted. As far as possible, the positive rhombencephalic populations were referred to their rhombomeric levels using the entry of cranial nerves and some nuclei as reference posts. The results of tract-tracing experiments from the spinal cord in this zebrafish transgenic line also reveal the location of GFP- positive neurons with respect to the well-characterized brain-spinal projecting populations. The nomenclature used for the reticulospinal populations is based on Lee and Eaton (1991) and Becker et al. (1997).

RESULTS

Study of adult brain and spinal cord sections of the Tg(*glyt2:gfp*) transgenic zebrafish line with fluorescence and confocal microscopy revealed the existence of abundant GFP-expressing neurons in the rhombencephalon and spinal cord. GFP-positive neurons were also observed in the midbrain and forebrain, and numerous positive fibers were observed in many brain regions. The distribution of these fluorescent populations and fibers is summarily represented in the chart of Figure 1.

In order to confirm that the GFP-fluorescent populations actually express GLYT2, we conducted *in situ* hybridization experiments with a GLYT2 probe in transgenic zebrafish, combined with GFP immunofluorescence. GLYT2-expressing neurons were observed only in the rhombencephalon and midbrain (Figs. 1-2), as detailed below. Additionally, the use of immunofluorescence with an anti-GFP antibody revealed the same cell populations and fibers that exhibited fluorescence in untreated brain sections of the transgenic fish, excluding thus false positive cells exhibiting non-specific autofluorescence.

For the study of GFP/GLYT2 coexpression in different neuronal populations, two different times for the histoenzymatic hybridization reaction were used (2h and overnight). The reaction product is fluorescent in the far red,

which allowed exploring GLYT2 expression together with GFP expression by confocal microscopy. Long reaction time (overnight) allowed revealing faint GLYT2 signal in small-celled neuronal populations including those of the facial and vagal lobes, although the *in situ* hybridization reaction product often obscured GFP fluorescence of larger neurons. Short reaction times (2h) revealed strong GLYT2 expression in large and medium-sized GFP-positive cells such as those of the rhombencephalic reticular formation but often failed to demonstrate signal in smaller cells. Clearly double-labeled neurons were observed in the medial nucleus of the octavolateral area, several primary octaval nuclei and the secondary octaval nucleus, as well as in the facial and vagal lobes and the reticular formation (see Figs. 3 and 4). These double labeling experiments also revealed discrepancies between expression of GFP and GLYT2 at the level of neuronal populations in the mesencephalon and prosencephalon, as well as in some rhombencephalic populations (see below).

In the following sections, we first describe the GFP-positive neurons and then the GLYT2-positive neurons for the various brain regions, indicating their relationship. We also describe the GFP-positive innervation observed, assuming the hypothesis that most GFP-positive fibers originate from double labeled GFP/GLYT2 neurons. Single GFP-positive neurons are very scarce in the brain by comparison with GLYT2-positive neurons. Accordingly, their contribution to the GFP-positive innervation of brain regions is probably insignificant compared with innervation by axons of the numerous populations that heavily express GFP and GLYT2 mRNA. Note that the axons of GLYT2 positive/GFP negative neurons would not be detectable with present methods.

Distribution of GFP-positive neurons and fibers and GLYT2-expressing perikarya in the Tg(*glyt2:gfp*) transgenic zebrafish

The figure 1 presents the distribution of putative (GFP-positive, GFP/ GLYT2-positive and GLYT2-positive) glycinergic cells and GFP-positive fibers. Photomicrographs of these GLYT2-positive cells are presented in Figure 2 and of GFP-positive cells and fibers are presented in Figures 3-7 and 9-13. Many cells of the GFP-positive rhombencephalic populations were also stained using glycine immunofluorescence in wild type zebrafish (Figures 14 and 15), which gives support to the idea that a part of the GFP-expressing cells

observed in the rhombencephalon also accumulate detectable levels of glycine in their perikarya (see discussion).

Prosencephalon

GFP expressing neurons

The telencephalon of adult zebrafish lacked GFP-positive cells (Fig. 1A-E). Some GFP-positive perikarya were observed in the hypothalamus and diencephalon proper of adult zebrafish. A fairly abundant population of small GFP-positive cells was observed in the periventricular region of the ventral hypothalamus, ventrally to the anterior tuberal nucleus (Figs. 1J, 5A). In the preglomerular complex, which is a group of migrated relay nuclei characteristic of teleosts, a small group of medium-sized GFP-positive cells (9-13 μm) were observed located dorsally to the medial preglomerular nucleus/tertiary gustatory nucleus complex and close to the posterior thalamic nucleus (Figs. 1-J, 5B), and occasional GFP-positive cells were also observed in this nucleus (not shown). This group lies rostro-dorsal to the midbrain nucleus with GLYT2-expressing neurons (see below). In the alar diencephalon, the periventricular pretectal nucleus and the pineal organ showed GFP-positive perikarya. The periventricular pretectal nucleus, located close to the posterior commissure, showed a few pale rounded fluorescent perikarya (Figs. 1H, 5C). The pineal organ of adult zebrafish, a long tubulo-vesicular neuroepithelial structure projecting rostrally from the roof of the pretectum, showed a large number of small GFP-positive cells (6.7 ± 0.8 μm, n=15) distributed along the entire vesicle (Figs. 1E, 5D-E). These cells exhibited basal processes coursing toward putative neuropil regions in the basis of the neuroepithelium (Fig. 5E). By their shape and connections, these cells appear to be pineal photoreceptor cells (pinealocytes). A small group of GFP-positive cells was also observed in the pineal stalk. No GFP-positive cell was observed in the small parapineal organ. None of the aforementioned populations showed detectable levels of GLYT2 mRNA.

GFP expressing fibers

The telencephalon showed some GFP-positive fibers. In the olfactory bulb, GFP-positive fibers were observed coursing in the granule cell layer and

close to olfactory glomeruli (Figs. 1A-B, 5F). In longitudinal sections, these fibers appear to reach the bulb coursing from the basal telencephalon (Fig. 5F). In the telencephalic lobe, scarce GFP-positive innervation was observed in central, medial and dorsal parts of the dorsal telencephalic area (Figs. 1C, 5G) and lateral regions intermediate between the dorsal and ventral areas (Figs. 1C-D, 5G-H), but fibers were mostly absent in other telencephalic regions. GFP-positive fibers coursed along the forebrain bundles and the entopeduncular region (Fig. 1D-E).

The hypothalamus lacked GFP-positive fibers in most regions, including the lateral torus and the lateral and posterior hypothalamic lobes (Fig. 1H-K). No obvious GFP-positive fiber plexus was related with the few tubercular cells that were labeled by the tracer from the spinal cord. The innervation of the preglomerular complex by GFP-positive fibers is very sparse. In the medial region of the thalamus, an oblique band of GFP-positive fibers was observed in the zona limitans intrathalamica (Figs. 1H, 5C), and some fibers were also observed in the ventral thalamus and posterior tubercle (Fig. 1G-I). GFP-positive fibers ascending in the lateral longitudinal fascicle gave rise to a conspicuous field of terminal fibers in the pretectal area lateral to the periventricular pretectal nucleus (Fig. 5C). From the pretectal area, a tract of thin GFP-positive fibers coursed rostro-ventro-medially, crossed the midline in a ventral postoptic commissure and projected to the magnocellular superficial pretectal nucleus (Figs. 1G, 6A, B), which was the only nucleus of this superficial region richly innervated by GFP-positive fibers (for characterization of this region see Castro et al., 2006a). From the pretectal region, too, rather thick fibers entered the rostral region of the optic tectum and coursed and branched along the tectum to form the four GFP-positive fiber plexuses (Figs. 1F-M, 6C-E, see also below). The conspicuous pineal tract of the zebrafish did not show GFP-positive fibers (for the connections of the zebrafish pineal, see Yáñez et al., 2009). In the basal synencephalon (prosomere 1), the nucleus of the medial longitudinal fascicle received moderate GFP-positive innervation (Figs. 1-J, 6F), and fibers formed some contacts with perikarya and dendrites of large cells, as shown in experiments of retrogradely labeling from the spinal cord (Fig. 6G-I).

Mesencephalon

GFP expressing neurons

The midbrain consists of a large dorsal region, the optic tectum, which covers the torus semicircularis and midbrain tegmentum. In the midbrain, the only GFP-expressing cells were observed in the medial region of the torus semicircularis (Figs. 1L, 7A, D, 8A-B). Here, some small GFP-positive cells (5.3 ± 0.2 µm, n=10) were observed in a small medial cell region that is continuous with the periventricular cell mantle of the central nucleus of the torus semicircularis (Wullimann et al., 1996). They were round pear-shaped neurons with a single process directed ventrolaterally toward a conspicuous glycinergic neuropil (Figs. 7A, D, 8B). This GFP-positive population was lateral to the lateral valvular nucleus, from which is separated by a small ventricular sulcus, and dorsolateral to the perilemniscal nucleus of Wullimann et al. (1996), as it can be appreciated in Nissl-stained sections (Fig. 8A). Because this nucleus does not project to the cerebellum, but ventrolaterally, it was concluded that it is not a part of the lateral valvular nucleus. No evidence of GLYT2 mRNA expression in this GFP-positive population was obtained.

GLYT2 expressing neurons

A small compact group of round perikarya expressing GLYT2 mRNA was observed in the lateral ventral tegmentum, just above the ansulate commissure (Fig. 2A), a major midbrain commissure of teleosts. No GFP-positive cells were observed at this level in transgenic fish using fluorescence microscopy. This small nucleus was not recognized in the zebrafish brain atlas (Wullimann et al., 1996).

GFP-positive fiber innervation

The optic tectum was innervated by GFP-positive fibers that coursed in the lateral longitudinal fascicle toward the pretectum, entering through the rostral tectum and branching and descending along the entire tectum forming four loose horizontal bands of GFP-positive fibers at the level of the stratum griseum et fibrosum superficiale (two bands), stratum griseum centrale and stratum album centrale (Figs. 1F-L, 6D-E). Very sparse GFP-positive fibers were observed in the outer region of the stratum griseum periventriculare. The torus longitudinalis, a cerebellar-like paired structure located in the tectal midline, did not exhibit GFP-positive fibers (Fig. 1G-J).

In a region ventromedial to the torus semicircularis, there was a characteristic neuropil formed of a rich plexus of beaded GFP-positive fibers (Figs. 1K-L, 7A). This GFP-positive fiber plexus extended in ventrorostral direction to a reticular region lateral to the perilemniscal nucleus, medial to the tectobulbar tract and over the ansulate commissure (Fig. 7B-F). This positive neuropil ended at the transition with the pretectal tegmentum (i.e. the level of appearance of the nucleus of the medial longitudinal fascicle). The region containing this neuropil is easily recognizable adjacent to the fiber-rich tectobulbar tract in transverse sections of the midbrain in the adult brain atlas (Wullimann et al., 1996), but it was unnamed. Whether this neuropil pertains to the torus semicircularis or should be considered a different structure is not known. Some of these fibers probably originate from toral GFP-positive neurons, but other origins such as hindbrain GFP-positive neurons could not be ruled out because thick GFP-positive fibers coursing in the lateral lemniscus (lateral longitudinal fascicle) give rise to fibers and collaterals to the torus. The other regions of the torus semicircularis are less densely innervated by GFP-positive fibers (Figs. 7A-B, 8B). In the medial region of the mesencephalic tegmentum, the ventromedial reticular area exhibited moderate GFP-positive innervation, and moderate GFP-positive fibers were observed in the oculomotor nucleus (Figs. 1J-K, 7C). Some GFP-positive fibers coursed in the medial and lateral longitudinal fascicles (Figs. 1J-K, 7A-C, F). These long ascending fibers arose probably from hindbrain GFP-positive neurons.

Rhombencephalon

The zebrafish rhombencephalon arises during development from a series of transverse segmental entities, the rhombomeres, which extend along most of its length. The rhombomere 0 corresponds to the isthmus, which contains the trochlear nucleus, the nucleus isthmi and the secondary gustatory/visceral nucleus, and rhombomere 1 gives rise in its dorsal region to the cerebellum. The ventral midline of rhombomeres 0 and 1 contains the interpeduncular nucleus of this rostral region. The rostral hindbrain region derived from these two first rhombomeres lacks any GFP-expressing neuron in the zebrafish, and this applies to the cerebellum. GFP-positive hindbrain neurons of the transgenic zebrafish were located between the rhombomere 2

and the caudalmost hindbrain. There were GFP positive neurons both in alar and basal plate-derived regions. Results with GLYT2 *in situ* hybridization in transgenic zebrafish (Fig. 2) reveal a similar pattern of neuronal distribution in the rhombencephalon, although some GLYT2-positive neurons were not observed by GFP fluorescence/immunofluorescence. The results of GLYT2 *in situ* hybridization will be described together with GFP results.

GFP-expressing and GLYT2-expressing neurons in the rhombencephalic alar region

Medial octavolateral nucleus

The medial octavolateral nucleus is located below the cerebellar crest that covers the octavolateral area and it contains numerous GFP-positive neurons (Fig. 1O-S). Two types of GFP-positive cells were observed in this nucleus (Fig. 9A-H). Some cells expressing GFP of this nucleus were rather pale and had spindle-shaped or triangular perikarya (8.9 ± 0.6 µm in diameter; n=11) that characteristically send long and slender dendrites (thickness in basal parts: 4.3 ± 0.3 µm, n= 6) to the cerebellar crest, where they branch moderately and progressively became thinner and paler (Figs. 1O-R, 9D, G). If these dendrites bear dendritic spines was not appreciated. These cells were identified as a type of crest cells. The number of these cells was higher at the level of the octaval and lateral line nerve entrances, and rostrally or caudally to this middle region only GFP-positive processes were observed. In addition, the medial nucleus exhibited a larger population of small brightly fluorescent GFP-positive globular neurons (6.4 ± 0.4 µm in diameter; n=11), which were observed through most of the rostrocaudal extension of the nucleus (Fig. 9A, C, E-G, H). Dendrites of these cells were thin and tortuous and coursed in the medial octavolateral nucleus. The medial nucleus itself contained a rather rich innervation by beaded GFP-positive processes (Fig. 9H), whereas the cerebellar crest mostly lacked GFP-positive axonal processes and only a few of these fibers enter in its basal region (Fig. 9G). Caudal to the Mauthner cell, the cerebellar crests of both sides are joined together splitting the fourth ventricle in dorsal and ventral regions and a fiber commissure can be appreciated below the crest. Thin GFP-positive axonal processes cross in this commissure (Figs. 1P-Q, 9E) and a few small GFP-positive cells were also interspersed with these

fibers. The small GFP-positive cells are the probable origin of these dorsal commissural fibers.

In situ hybridization reveals the presence of abundant GLYT2 neurons in the medial octavolateral nucleus (Figs. 2E-H, 3B-C). Results of GFP/GLYT2 double labeling experiments confirmed the presence of two types of double labeled perikarya corresponding to the two main types of GFP-positive cells described above. These cells were intermingled with GFP-only and GLYT2-only perikarya (Fig. 3A-C), indicating that colocalization was not obvious in all putative glycinergic cells.

Primary octaval nuclei

The ventral zone of the octavolateral region receives primary octaval (vestibular) fibers and consists of five differentiated parts, the anterior (AON), magnocellular (MaON), tangential, descending (DON) and posterior octaval nuclei (Wullimann et al., 1996). Previous experimental studies showed that some cells in these nuclei have spinal projections (Becker et al., 1997). The anterior, magnocellular and tangential nuclei were heavily labeled by retrograde transport from the spinal cord in our current experiment (see Fig. 9A-D, H), which facilitated the topological analysis of GFP-positive cells and processes in this region. A conspicuous compact group of spindle-shaped GFP-positive cells (minor axis 10.7 ± 0.4 µm, n=10) was observed medially to the spinal-labeled AON and MaON neurons, between these nuclei and the Mauthner cell (Figs. 1O-P, 9A-C). This cell group appears to give rise to the very conspicuous commissural tract of thick GFP-positive fibers (diameter 5.1 ± 1.3 µm, n=15) that contact the Mauthner cell perikarya by thin collaterals (see below). Caudally, this group is replaced by a more loose population of small GFP-positive cells located in the medial and dorsomedial region of the spinal-projecting MaON neurons at the level of the octaval nerve entrance. In the descending octaval nucleus, GFP-positive cells were observed in similar position although caudally its number diminishes progressively (Figs. 1Q-R, 9E). Ventrally to this group and dorsomedially to the secondary gustatory tract, there is a more compact group of larger GFP-positive cells. These cells give rise to a conspicuous fascicle of GFP-positive dendrites coursing ventrolaterally and rostrally. A number of GFP-positive commissural fibers

appear to arise from the AON/MaON-associated GFP-positive populations, and GFP-positive axons and boutons also appear to contact perikarya and dendrites of these nuclei (Fig. 9H). The region of the tangential nucleus did not show GFP-positive cells (Figs. 1Q, 9C), and the nucleus only shows sparse GFP-positive fibers.

GLYT2 expression was observed in numerous cells of the primary octaval nuclei in locations corresponding to the aforementioned GFP-positive neurons. These include the anterior (Fig. 2E-F), magnocellular (Fig. 2E-F), descending (Fig. 2G-H) and tangential (Fig. 2G) octaval nuclei. Double labeling was observed in the combined experiments in cells of most of these primary octaval populations (see Fig. 3D-F), although the presence of GFP-only and GLYT2-only perikarya indicates that colocalization was partial. Noticeably, cells of the tangential nucleus (a crossed spinal projecting octaval nucleus of teleosts) were GLYT2 positive but GFP negative (Fig. 3G-I).

Secondary octaval nucleus

The secondary octaval nucleus is located medially near the ventricular surface and receives fibers from some primary octaval nuclei (Wullimann et al., 1996). It contained pale rounded GFP-positive cells (10.8 ± 1.5 µm, n= 5) that were mainly located in ventral regions of the nucleus (Figs. 1O-P, 9A-C, I). These cells extended dendrites in the nucleus, which contains scarce number of GFP-positive processes, gave rise to arcuate fibers and commissural GFP-positive fibers also appear to contact with this nucleus. The origin of afferent commissural fibers could not be assessed.

Abundant GLYT2-expressing neurons were also observed in the secondary octaval nucleus (Fig. 2F-G). Double labeling revealed colocalization of both GFP and GLYT2 mRNA in numerous perikarya of this nucleus (Fig. 3J-L). The dense dark blue NTB/BCIP reaction product, however, obscured GFP immunofluorescence in a part of these neurons.

Viscerosensory lobes

The viscerosensory region of the zebrafish is subdivided into three lobes, one rostral and unpaired (facial lobe), a smaller and paired intermediate lobe (glossopharyngeal lobe) and a large paired caudal lobe (vagal lobe).

Numerous small, pear-shaped GFP-expressing perikarya (facial lobe, 5.5 ± 0.3 µm, n= 15; vagal lobe, 6.2 ± 0.5 µm, n=15) were observed mostly in the superficial (cellular) layer of the viscerosensory lobes, but some were also located inside the central neuropil region, both in the vagal and facial lobes (Fig. 1R-W, 10A-E). Typically, 40-50 GFP-positive neurons per 25-µm-thick section were observed in the vagal lobe and 40-80 cells (on both sides of the midline) in the unpaired facial lobe. There, cells were scattered among a larger population of negative cells (Fig. 10D,E). Thin processes of these cells coursed to the inner neuropil region where they appear to give rise to a large number of small bouton-like structures scattered rather homogeneously throughout the facial lobe, and concentrated in superficial regions in the vagal lobe. No obvious GFP-positive projection from the lobes on the facial-vagal motor column was noted. Judging from the scarce GFP-positive processes observed in the visceromotor column and in the secondary gustatory/visceral nucleus and tract, most processes of these GFP-positive neurons probably form part of local circuits of the visceral lobes. The caudal part of the viscerosensory column that includes the commissural nucleus (general visceral region) showed very few small GFP-positive neurons (Fig. 10C), and the area postrema showed no glycinergic structures (Fig. 1X).

In the facial and vagal lobes, numerous GLYT2-positive neurons were observed (Figs. 2H-I, 4B-C). Double labeling experiments revealed partial colocalization of GFP and GLYT2 mRNA in perikarya (Fig. 4A-C). The amount of GLYT2 reaction product observed, even after long incubation (see material & methods) in most cells was small and often was restricted to a small or very small conic part of the perinuclear cytoplasm (Fig. 4B-C). In a part of the GLYT2 positive neurons of the viscerosensory lobes, no GFP signal was detected in these experiments (Fig. 4A-C). The area postrema lacked GLYT2 positive neurons (Fig. 2J).

GFP-expressing neurons in the rhombencephalic basal region

Motor nuclei

A few GFP-positive neurons were observed at the level of the glossopharyngeal and vagal motor nuclei (Figs. 1T-W, 11H). These cells occupy a position somewhat lateral to the motoneurons demonstrated in

zebrafish in studies using immunohistochemistry against choline acetyltransferase (Clemente et al., 2004; Mueller et al., 2004). These cells extended dendrites in the same ventrolateral region as the dendrites of motoneurons. *In situ* hybridization also revealed GLYT2 expression in neurons of this region (Fig. 2I).

Reticular region

The zebrafish rhombencephalic reticular regions exhibit well-characterized groups of reticulospinal neurons that show a clear segmental organization in larvae (Kimmel et al., 1982; Metcalfe et al., 1986). Here, the location of reticulospinal populations labeled by tract-tracing from the spinal cord were used to analyze the distribution of GFP-positive neurons and fibers. The superior reticular region that contains the Ro1 group (rhombomere 1) does not contain GFP-positive cells although *in situ* hybridization reveals the presence of some GLYT2 positive perikarya in this region. The most rostral GFP-positive cells of the rhombencephalic reticular region are small neurons scattered ventral to the Ro2 group (rhombomere 2) (Figs. 1N, 11A), and caudally GFP-positive cells become more numerous, consisting of small positive cells located below and intermingled with larger GFP-negative reticulospinal cells (Fig. 11B). None of the cells of the superior reticular formation labeled from the spinal cord were GFP positive. A dorsal cluster of small GFP-positive cells was observed just caudal to the dorsal trigeminal motor nucleus (Fig. 11B; level not represented in Figure 1). Comparatively more abundant GLYT2 mRNA-expressing perikarya were observed in all these locations using *in situ* hybridization (Fig. 2B-D), and combined experiments revealed the presence of some GFP/GLYT2 double labeled perikarya (not shown).

In the intermediate reticular formation, numerous small to medium sized GFP-positive neurons were observed closely related to the large reticulospinal and raphe-spinal cells of this region (Fig. 1O-R). Tract-tracing experiments in transgenic zebrafish indicate that these GFP-positive cells were found intermingled with, dorsal to and lateral to reticulospinal cells, most of them caudally to the Mauthner cell (Figs. 1P-R, 11C-F). In addition, a more ventral and compact group of small GFP-positive cells (Figs. 1Q, 11E) was

observed over the region of the abducens nucleus, which occupies a ventral location near the meninges (as determined by Clemente et al., 2004 and Mueller et al., 2004). Whether these cells are reticular neurons or interneurons associated to this motor nucleus was not determined.

In the inferior reticular formation, at least 4-6 perikarya of GFP-positive reticular cells were observed on each side in all transverse sections in which the facial and vagal lobes were present (Figs. 1S-W, 11H-I). These spindle-shaped cells are located just lateral to the medial longitudinal fascicle and extend long dendrites ventrally and ventrolaterally. Commissural GFP-positive axons probably originated from these cells were observed along all the extension of the inferior reticular formation.

In situ hybridization results indicate that GLYT2-positive perikarya are numerous in the intermediate and inferior reticular region (Fig. 2E-I), including some positive cells in the inferior raphe nucleus (Fig. 2H) and cells displaced ventrolaterally near the abducens nucleus (Fig.2G-I). Combined *in situ* hybridization and immunofluorescence revealed the presence of abundant GLYT2/GFP-positive neurons in the reticular formation (Fig. 4D-F), although the presence of GFP-only and GLYT2-only labeled cells indicate partial coexpression of these markers. Cells apparently expressing GLYT2 only were rather abundant (Fig. 4D-F), probably due to masking of GFP fluorescence by the dense dark blue NTB-BCIP reaction product. Interestingly, the three characteristic GFP-positive spinal-projecting large reticular neurons, expressed GLYT2 mRNA. In these cells GFP immunofluorescence was intense whereas GLYT2 signal was comparatively faint (Fig. 4G-I), facilitating identification of these cells. These cells are described below in detail.

Large GFP-expressing reticular neurons project to the spinal cord

Three pairs of large GFP-positive cells projecting to the spinal cord via the dorsal part of the medial longitudinal fascicle and located caudal to the Mauthner cell were identified in present tract-tracing experiments (Figs. 1P-R, 11D-F). Each pair of cells exhibits differential features. The rostralmost spinal-projecting GFP-positive cell pair is located in a medial group of spinal-projecting reticular neurons that are just caudal to the Mauthner cells at the transverse level of the secondary octaval nucleus and lateral to the ventral part

of the medial longitudinal fascicle (Figs. 1P, 11D). This rostral pair exhibits oval perikarya and a long ventrolateral dendrite that bifurcates one or two times. The axons coursed to the dorsal part of the medial longitudinal fascicle surrounding dorsally the Mauthner axons. The second pair of spinal-projecting GFP-positive cells (Figs. 1Q, 11E) is located at the transverse level of the most rostral part of the facial lobe, lateral to the medial longitudinal fascicle and just rostral to the decussation of axons of the tangential nucleus labeled by the tracer from the spinal cord. These GFP-positive cells show a conspicuous perikaryon with thick dorsolateral and ventral dendrites and a rather thick axon coursing to the dorsal part of the medial longitudinal fascicle, crossing the midline and coursing caudally. The third pair of spinal-projecting GFP-positive cells (Figs. 1R, 11F) is located more caudally at a level slightly rostral to the conspicuous raphe-spinal neurons that were labeled from the spinal cord, at the rostral level of the glossopharyngeal lobe. These cells show spindle-shaped perikarya with a thick ventral dendrite branching several times and a dorsal axon coursing to the dorsal part of the medial longitudinal fascicle and crossing the midline below the Mauthner axons. The thick GFP-positive axons of these three pairs of cells coursed to the spinal cord in the dorsal part of the medial longitudinal fascicle, close to the giant Mauthner axon (Figs. 1Q-X, 11E-I).

In addition to these conspicuous cells, occasional small spinal-projecting spindle-shaped GFP-positive cells were observed in the reticular region (Fig. 11E), at the levels of the Mauthner cell (not shown) and in the inferior raphe nucleus (Fig. 11G).

GFP-positive innervation of other rhombencephalic structures

Glycinergic innervation of the Mauthner cell

The Mauthner cell (MC) receives rich innervation from GFP-positive fibers, as revealed in experiments of tract-tracing from the spinal cord (Fig. 12). The most striking and dense contacts came from a very conspicuous commissural bundle of thick GFP-positive axons (5.1 ±1.3 µm in diameter without myelin sheath; n= 15) (Figs. 1O, 12A-D, I-K). These fibers coursed over and toward the MC. These thick fibers originated from the group of GFP/GLYT2-positive cells located close to the AON and MaON at the entrance level of the octaval nerve (see above). In the neighborhood of the MC

axon cap, these fibers formed several thinner branches and together coursed as a sleeve at the border of the axon cap to make massive contacts on the perikaryon around the axon hillock region (Fig. 12B, I-K). Small GFP-positive boutons were also scattered on the surface of Mauthner cell dendrites, including the very thick ventral and lateral dendrites (Fig. 12E-H) and on other regions of the perikaryon, but these GFP-positive boutons were rather sparse by comparison with those innervating the region of the axon hillock.

Cerebellum

The zebrafish cerebellum consists of a cerebellar body, paired granular eminences and a cerebellar valvula that is invaginated into the mesencephalic ventricle. No cells expressing GFP (Fig. 1H-P) or GLYT2 (not shown) were observed in these cerebellar regions. Moreover, commissural fibers crossing in the cerebellar commissure at isthmus level were the only GFP-positive fibers observed in the cerebellum of the transgenic zebrafish. These fibers did not enter cerebellar layers (molecular layer, Purkinje cells, eurydendroid cells and granule cell layer).

Isthmus

The zebrafish isthmus contains some characteristic nuclei: a big secondary gustatory nucleus and a smaller nucleus isthmi, dorsally, and the trochlear nucleus and interpeduncular nucleus, ventrally (Fig. 1L-M). The secondary gustatory nucleus showed a loose plexus of very thin GFP-positive fibers in ventral and lateral parts, whereas the nucleus isthmi showed a few GFP-positive boutons in the core neuropil. GFP-positive innervation was more abundant in the central gray, locus coeruleus and reticular areas, but very scant in the interpeduncular nucleus. Some GFP-positive fibers coursed longitudinally throughout this region in the medial and lateral longitudinal fascicles.

Caudal medulla and transition to the spinal cord

In transverse sections of the most caudal medulla and rostral spinal cord, GFP-positive cells were observed both in dorsal and ventral regions (Fig. 13A-D). Fairly numerous small GFP-positive cells were observed in the medial

funicular nucleus, mostly ventromedially (Fig. 13A-C). These cells send long dendritic processes to neuropil areas of the nucleus. Larger GFP-positive cells were observed laterally and ventrolaterally to the central canal, in a dorsal region of the ventral horn (Fig. 13A-D). Numerous GFP-positive processes were observed in the ventral horn region occupied by motoneuron perikarya and in the ventral part of the lateral funiculus to which motoneurons send abundant dendritic processes (for description of cholinergic motoneurons, see Clemente et al., 2004; Mueller et al., 2004). Fairly abundant GFP-positive axons crossed the midline in the ventral commissure that separates the medial longitudinal fascicle into dorsal and ventral parts (Fig. 13A-D). With regard to GLYT2 mRNA expression, numerous positive perikarya were observed in the rostral spinal cord in locations comparable to those of GFP-positive cells (Fig. 2J), and GFP/GLYT2 double labeled neurons were also observed in these locations (not shown).

The most conspicuous GFP-positive axons in the spinal cord were the three pairs of thick axons coursing in the medial longitudinal fascicle dorsally to the Mauthner axons (Fig. 13A-D). The other fibers of the mlf, both in the dorsal and ventral regions, lacked GFP-positive expression. A very conspicuous GFP-positive tract was observed in ventrolateral position near the meninges (Fig. 13A-D). This tract was also observed in similar position in rhombencephalic levels until the level of the octaval nerve entrance (Fig. 1Q-W).

Glycine immunofluorescence

In order to investigate the presence of glycine in neuronal populations containing GFP-positive and/or GLYT2-positive cells observed in the transgenic zebrafish, we used glycine immunofluorescence in sections of wild-type zebrafish brains. This procedure revealed the presence of glycine-immunoreactive (-ir) neurons and fibers in various nuclei that in the transgenic zebrafish also showed GLYT2 and/or GFP-positive cells, although the procedure yielded good immunoreaction only in rather superficial brain structures. In these superficial regions, the distribution and appearance of positive cells in wild-type zebrafish was comparable with those of GFP-expressing cells in the same regions of transgenic zebrafish, although the poor

penetration of the antibody in the glutaraldehyde-fixed sections led to staining of structures only in a few micrometers deep in the surface of the section. These methodological shortcomings precluded to compare one-by-one the glycine-ir cell populations with the GFP fluorescence and GLYT2 positive populations of the transgenic fish. Accordingly, glycine immunoreactivity will be described only in selected nuclei and regions.

The distribution of glycine-ir fibers observed in the olfactory bulb (fibers mainly in a region close to the glomerular layer, Fig. 14A), telencephalon (few fibers coursing in the pallium or dorsal telencephalic area, Fig. 14B), pretectal area (mostly passing toward the optic tectum (Fig. 14C) and optic tectum (numerous fibers showing a layered distribution, Fig. 14C-D) was similar to that reported above for GFP-positive fibers. Examples of the neuronal populations revealed by glycine immunohistochemistry are presented in the Figures 14E-F and 15. Some small glycine-ir cells were located medially in the central nucleus of the torus semicircularis (Fig. 14E). In the rhombencephalon, the medial octavolateral nucleus showed abundant glycine-ir neurons, both of crest cell type and more basal small cells (Fig. 14F). Glycine-ir neurons were also observed in primary octaval nuclei (Fig. 15A), the secondary octaval nucleus (Fig. 15B), and the facial and vagal lobes (Fig. 15C). In these nuclei, the morphology and relative abundance of glycine-ir cells were roughly similar to those of GFP-positive cells reported in the transgenic fish, but cell morphology and abundance was much better demonstrated by GFP fluorescence/immunofluorescence. The scarce glycine-ir cells observed in the reticular formation (Fig. 15D) were located in the same region containing GFP- and GLYT2-positive cells in the transgenic zebrafish. Some glycine-ir cells were also observed in the medial funicular nucleus and the ventral horn of the spinal cord (Fig. 15D-E).

DISCUSSION

General considerations

The present study reveals for the first time the distribution of glycinergic neurons and fibers in the brain of the adult zebrafish by using a Tg(*glyt2:gfp*) transgenic construct expressing the green fluorescent protein (GFP) under control of the GLYT2 regulatory sequences (McLean et al.,

2007). This study expands our knowledge on the glycinergic system of zebrafish obtained in studies of embryos and early larvae using GLYT2 *in situ* hybridization (Higashijima et al., 2004a,b,c) and Tg(*glyt2:gfp*) transgenic lines (McLean et al., 2007; Liao and Fetcho, 2008; Kinkhabwala et al., 2011; Koyama et al., 2011; Moly and Hatta, 2011).

The expression of GLYT2 is considered as a marker specific of glycinergic neurons (Zafra et al., 1995a,b; Poyatos et al., 1997; Zeilhofer et al., 2005). Present *in situ* hybridization results in adult Tg(*glyt2:gfp*) transgenic zebrafish reveal GLYT2 expression in most GFP positive neuronal populations, in which at least a part of neurons showed GFP/GLYT2 double labeling, which supports the use of this transgenic line for study of the adult glycinergic system. All the GLYT2 positive cells reported here are considered to represent glycinergic neurons. Although in general the distribution of GLYT2 mRNA and GFP fluorescence in the transgenic zebrafish showed good correspondence and it was possible to colocalize both signals in numerous neurons of the rhombencephalon and spinal cord, GLYT2 signal was not observed in any GFP positive neuron in other brain regions. This unexpected finding suggests that the correspondence between the GFP positivity observed in the transgenic zebrafish line and a glycinergic nature may not apply to some neurons. Since the two substances detected by GFP fluorescence/immunofluorescence and GLYT2 *in situ* hybridization are very different (a stable protein and a short-lived RNA, respectively), it is conceivable that they may have very different turnover in the cell. Thus, a possible explanation for the observation of GFP-positive/GLYT2-negative cells is that GLYT2 mRNA amounts were below the level of detection by down regulation of GLYT2 gene expression at the time of sacrifice. In the pineal organ of zebrafish and mammals transcriptional down regulation of some genes related to daytime has been reported (Pierce et al., 2008; Vatine et al., 2009; Rovsing et al., 2011). Whether this might apply to GLYT2 expression in the GFP-positive pineal cells is not known. Low or very low mRNA levels produced by small cells would also explain why long time reaction does reveal much GLYT2 expression in small cells of some hindbrain nuclei (vagal lobe, medial octavolateral nucleus) than short incubation times. On the other hand, the accumulation in the cell of a stable protein, even if

synthesized at very low rates, would facilitate its detection. The finding of glycine immunoreactivity in cells of the central nucleus of the torus semicircularis, which shows GFP-positive cells in the transgenic zebrafish, would support their glycinergic nature despite that apparently they were GLYT2 negative. Anyway, the possibility that GFP-positive/GLYT2-negative cells do express ectopically GFP cannot be ruled out. Leaky expression of GFP driven by the promoter has been suspected in transgenic zebrafish to explain the apparent disparity between expression of GFP and engrailed mRNA in the spinal cord (Higashijima et al., 2004c), and GFP and TH in the retina (Meng et al., 2008).

Additional evidences support the use of GFP fluorescence in the Tg(*glyt2:gfp*) zebrafish to study the adult glycinergic system. Glycine immunofluorescence in the adult brain of wild-type zebrafish revealed a pattern of positive neurons very similar to that observed with GFP in the transgenic fish, although one-to-one comparison of populations was only possible in superficially located nuclei owing to shortcomings of the glycine immunohistochemistry. In zebrafish embryos, Moly and Hatta (2011) also showed that the early pattern of glycinergic neurons and fibers revealed by glycine immunohistochemistry in the rhombencephalon was similar to that expressing GFP in the Tg(*glyt2:gfp*) embryos. Moreover, physiological studies in larvae of the Tg(*glyt2:gfp*) transgenic zebrafish confirmed that hindbrain GFP-expressing neurons were glycinergic inhibitory (Koyama et al., 2011). As noted in larvae and adults of these stable Tg(*glyt2:gfp*) transgenic lines GFP was only expressed by neurons, without any positive signal in glial cells.

In adult zebrafish, few GFP-positive neurons were observed in the diencephalon and mesencephalon, and most GFP-positive and glycine-ir cells were located in the rhombencephalon and spinal cord, the only glycinergic cells-containing regions reported in larvae (Higashijima et al., 2004a; Kinkhabwala et al., 2011; Koyama et al., 2011). Interestingly, the observed distribution of GFP-positive cells and fibers in adult zebrafish was very different from those reported with markers of GABAergic (Castro et al., 2006a, 2006b; Mueller et al., 2006; Mueller and Guo, 2009), cholinergic (Clemente et al., 2004; Mueller et al., 2004), catecholaminergic (Ma, 1997; Filippi et al., 2010; Yamamoto et al., 2010), serotonergic (Kaslin and Panula, 2001) and

histaminergic (Kaslin and Panula, 2001) systems. In larval zebrafish, the prospective glutamatergic and glycinergic neurons were also different (Higashijima et al., 2004a). Together, these observations provide further support for the specific expression of GFP in glycinergic cells of adults of this Tg(*glyt2:gfp*) line. The results of neuronal distribution obtained in this zebrafish transgenic line were in good agreement with the neuronal distribution of GLYT2 reported in *Xenopus* early tadpoles (Wester et al., 2008) and in transgenic mice (Zeilhofer et al., 2005).

In this study, the use of experimental animals in which a tracer was applied into the spinal cord allowed a detailed analysis of glycinergic structures in the brain stem, including the demonstration of the existence of individually identifiable reticulospinal glycinergic cells and the pattern of innervation of Mauthner cells by glycinergic fibers in adults. Finally, this very first comprehensive study of the glycinergic cells in an adult teleost allowed comparison with the glycinergic system of the sea lamprey and the Siberian sturgeon from a comparative perspective.

Comparison with developmental studies in zebrafish, lamprey and *Xenopus*

Studies in early larvae of zebrafish (4-5 days post-fertilization; dpf) have revealed that GLYT2 expressing neurons in the brain were restricted to the rhombencephalon, with a sharp boundary of expression that appear to lie near the border of rhombomeres 1 and 2 (Higashijima et al., 2004a). The rostral expression of GFP populations in larvae of the Tg(*glyt2:gfp*) transgenic line was also little rostral to the Mauthner cell (Koyama et al., 2011), and the pattern showed good correspondence with results using *in situ* hybridization (Higashijima et al., 2004a). These results are similar to that observed here for the rhombencephalon of adult zebrafish, which lacks GLYT2/GFP-expressing cells in the isthmus and first rhombomere. In contrast to these early larvae studies, GLYT2 expression was observed in a small midbrain tegmental nucleus and GFP expression was observed in some neurons of the mesencephalon (torus semicircularis) and diencephalon (pineal organ, periventricular pretectum and periventricular ventral hypothalamus), which probably indicates that these putative glycinergic neurons develop late in

development. In *Xenopus,* GLYT2 is expressed in forebrain cells quite late, judging from *in situ* hybridization results of Wester et al. (2008). Studies of the glycinergic rhombencephalic populations in early zebrafish larvae have indicated an organization in longitudinal columns or stripes extending dorsoventrally (Higashijima et al., 2004a; Kinkhabwala et al., 2011; Koyama et al., 2011). Such a columnar pattern was not clearly defined in the *Xenopus* hindbrain with GLYT2 *in situ* hybridization (Wester et al., 2008). A longitudinal columnar organization of glycinergic cells was also observed in the rhombencephalon of prolarvae of the sea lamprey (Villar-Cerviño et al., 2009), although in later stages glycinergic populations could also be assigned to specific nuclei and columns (Villar-Cerviño et al., 2008a, 2009). Present results in Tg(*glyt2:gfp*) transgenic adult zebrafish indicate that postembryonic columns give rise to multiple and characteristic GLYT2/GFP-expressing populations associated to sensory, motor and reticular regions. Although the correspondence of embryonic and adult glycinergic rhombencephalic populations could not be analyzed in detail, it seems that glycinergic cells originated in lateral columns or stripes populated octavolateral (medial octavolateral nucleus, octaval nuclei) and viscerosensory (facial, glossopharyngeal and vagal lobes) centers, whereas those originated in more medial columns gave rise to medial populations (motor nuclei-associated and reticular glycinergic neurons).

Comparison of glycinergic populations of adult zebrafish brain and other vertebrates

Forebrain

Significant differences in regional distribution were observed between putative (GFP-positive) glycinergic populations in adult zebrafish and the populations reported in the forebrain of lamprey (Villar-Cerviño et al., 2008a, 2009) and sturgeon (Adrio et al., 2011). Whereas glycine-immunoreactive neurons have been observed in the olfactory bulb of lamprey and sturgeon, GLYT2 or GFP-expressing cells are absent there in Tg(*glyt2:gfp*) transgenic zebrafish. Owing to the presence of GFP-positive and glycine-ir fibers (present results) and glycine receptor-expressing neurons (Imboden et al., 2001) in the

zebrafish olfactory bulb, possible effects of glycine could be mediated by projections of extratelencephalic neurons.

Abundant GFP-expressing cells were observed in the transgenic zebrafish pineal organ but similar glycine-immunoreactive cells were not mentioned in both lamprey and sturgeon (Villar-Cerviño et al., 2008a, 2009; Adrio et al., 2011). The presence of immunoreactivity for the vesicular inhibitory amino acid transporter (VIAAT or VGAT), involved in the transport of glycine and/or GABA, has been reported in the rat pinealocytes (Redecker et al., 2001). These cells release important amounts of glycine in vitro under stimulation, which suggested that glycine is a paracrine signal used in the pineal body of rodents (Redecker et al., 2001). The presence of high levels of expression of NMDA receptors and glycine transporter has also been reported in the rat pineal body (Sato et al., 1993). Our finding of GFP expression in Tg(*glyt2:gfp*) transgenic zebrafish pinealocytes appears consistent with these findings, suggesting that glycine may be used by pineal photoreceptors as a neurotransmitter or paracrine signal. However, the reasons of the lack of GLYT2 expression in these putative glycinergic cells need to be investigated.

No pretectal population similar to that expressing GFP observed in the Tg(*glyt2:gfp*) zebrafish has been found in adult sea lamprey with glycine immunohistochemistry (Villar-Cerviño et al., 2008a), although in prolarval lampreys transient glycinergic pretectal cells were observed (Villar-Cerviño et al., 2009). The pretectal glycinergic cells of the Siberian sturgeon occupy a position close to the fasciculus retroflexus (Adrio et al., 2011) and may correspond with those GFP-expressing cells observed in zebrafish. Glycinergic cells have been observed in the thalamus of lamprey (Villar-Cerviño et al., 2008a, 2009) and sturgeon (Adrio et al., 2011), but comparison with GFP-positive populations observed in the transgenic zebrafish diencephalon (close to the tertiary gustatory nucleus and the medial preglomerular nucleus) is obscured by the uncertain thalamic origin of these nuclei. Putative glycinergic populations in the periventricular hypothalamus have been observed in sturgeon (Adrio et al., 2011), zebrafish (present results) and in prolarval lamprey (Villar-Cerviño et al., 2009), but not in adult lamprey (Villar-Cerviño et al., 2008a). Judging from published photomicrographs by Wester et al. (2008), in swimming tadpoles of *Xenopus* there are two diencephalic

populations, dorsal and ventral, expressing GLYT2. In the forebrain of rodents, glycinergic cells were observed with glycine immunohistochemistry in the lateral habenula and subfornical organ (Rampon et al., 1996) and in GLYT2-EGFP transgenic mice in the posterior hypothalamus (Zeilhofer et al., 2005). These GLYT2 results in other vertebrates are in contrast with the apparent lack of GLYT2 expression in any cell of the zebrafish forebrain.

Midbrain

The zebrafish midbrain contains a single putative glycinergic population (GFP-expressing in the transgenic and glycine-ir in the wild type fish) in a medial region of the torus semicircularis, whereas GFP-expressing neurons are absent in other midbrain structures. We consider this putative glycinergic group as a part of the torus semicircularis because of its continuity with periventricular layer of the central toral nucleus (TSc), and by their ventrolateral projections. In the atlas of the adult zebrafish brain (Wullimann et al., 1996), this unnamed region was included in the lateral nucleus of the valvula. However, these cells lack projections to the cerebellum, which are highly characteristic of the lateral valvular nucleus of teleosts (see Yang et al., 2004). This medial toral population containing glycine-ir neurons gives rise to the adjacent rich GFP-positive neuropil that extends ventrolaterally in the tegmentum, and could correspond to an unreported toral subnucleus consisting of local projection neurons, unlike the central nucleus of the torus semicircularis.

Comparison with topography and cytoarchitecture of the TS of goldfish and carp revealed in experimental studies (Yamamoto and Ito, 2005) suggests that this small toral region of zebrafish corresponds with a medial portion of the TSc of in these fishes (acoustic region; see also McCormick and Braford, 1988).. Present results suggest differential specialization of putative glycinergic circuits in the lateral line (mechanoreceptive) and acoustic (sound receptive) regions of the zebrafish TS. Instead, the distribution of glutamic acid decarboxylase (GAD, the GABA synthesizing enzyme) and GABA show no obvious preference for any part of the TS in zebrafish (Castro et al., 2006b) and toadfish (Edds-Walton et al., 2010), respectively. Glycinergic neurons were reported in the torus semicircularis of lamprey (Villar-Cerviño et al., 2008a, 2009) but not in that of sturgeon (Adrio et al., 2011). Glycinergic cells were

also observed in the inferior colliculus of rodents (Zeilhofer et al., 2005), i.e. in the torus semicircularis homologue of mammals. Glycinergic neurons are present in the optic tectum in lamprey and sturgeon (Villar-Cerviño et al., 2008a, 2009; Adrio et al., 2011), but probably not in zebrafish (present results). Glycinergic (GFP/glycine-positive) innervation of the optic tectum observed in zebrafish appears to arise from rhombencephalic neurons, as a difference with sea lamprey and sturgeon. Expression of glycine receptor mRNAs has been reported in the zebrafish optic tectum (Imboden et al., 2001), which is consistent with the observed glycinergic innervation.

In situ hybridization reveals the presence of a small glycinergic nucleus in the ventral tegmentum of adult zebrafish. Although a midbrain population of GLYT2-expressing cells was reported in *Xenopus* tadpoles of stages 35-37 (Wester et al., 2008), its assignation to the midbrain should be confirmed in adult brain.

Hindbrain

The absence of glycinergic (GFP and/or GLYT2-expressing) populations in the rostral rhombencephalon (cerebellum, isthmus and first rhombomeres) of the Tg(*glyt2:gfp*) zebrafish is similar to that reported with glycine immunohistochemistry in the sturgeon (Adrio et al., 2011), suggesting that this pattern is shared by actinopterygian lines. Instead, in the lamprey the rostral rhombencephalon contains numerous glycinergic neurons organized in basal and alar nuclei (Villar-Cerviño et al., 2008a, 2009). This notable difference suggests that glycinergic systems in agnathans and gnathostomes followed different evolution, either by loss of ancestral populations in the rostral rhombencephalon in early gnathostomes or acquisition of these populations in lampreys after separation of jawed and jawless vertebrates. In the sea lamprey, this rostral rhombencephalic region appears to be involved in motor coordination (see Villar-Cerviño et al., 2008a, 2009), which suggests that neurochemical mechanisms of control of premotor centers have changed in the two main lines of vertebrates. The high bending of this region in mammals complicates comparison of our results in zebrafish with those reported in the rat (Rampon et al., 1996). Anyway, the scant glycine-immunoreactive neurons observed in figures of this rat study that show pontine nuclei and the interpeduncular nucleus in transverse sections, and those that show the locus

coeruleus and the dorsal and dorsolateral tegmental nuclei (all of them derived from the rostral rhombencephalon), suggest a similarity with our zebrafish results. This is similar to that observed in the rostral rhombencephalon of sturgeon (Adrio et al., 2011). Accordingly, results in sturgeon, zebrafish and rat suggest a common absence or scarcity of glycinergic populations in the rostral rhombencephalon of jawed vertebrates.

The cerebellum contains glycinergic neurons in frog and mammals (Reichenberger et al., 1993; Zeilhofer et al., 2005), but not in sturgeon (Adrio et al., 2011) and zebrafish (present results). This notable difference suggests that the acquisition of glycinergic cells in lines leading to tetrapods occurred after their separation from lines of ray-finned bony fishes. Note that lampreys lack a true cerebellum (see Lannoo and Hawkes, 1997), which precludes comparison with gnathostomes.

In rodents, glycinergic neurons were abundant in the rhombencephalon, mainly in the reticular formation, in various nuclei of the auditory system, in vestibular nuclei, and in the spinal trigeminal complex (Rampon et al., 1996; Zeilhofer et al., 2005). This distribution is only roughly similar to that of GFP/GLYT2-positive cells observed in the reticular formation of Tg(*glyt2:gfp*) zebrafish. The medullary auditory nuclei of zebrafish show notable anatomical differences with auditory centers of mammals, because teleosts lack a clear distinction between vestibular and acoustic (cochlear) primary centers, as well as lacking a recognizable superior olive-trapezoid corpus nuclear complex. The dorsal part of the descending octaval nucleus, the anterior octaval nucleus and the secondary octaval nucleus are the most important auditory centers in the teleost medulla (see Edds-Walton et al., 1999, 2010), and all of them exhibit glycinergic cells and a rich glycinergic fiber plexus (present results). The presence of GABAergic cells and/or fibers in these nuclei has been reported in the toadfish (Edds-Walton et al., 2010), indicating that both inhibitory neurotransmitters (glycine and GABA) are used in auditory circuits. In the secondary octaval nucleus of some teleosts, three different neuronal populations have been described, two regions of fusiform cells and one region of spherical cells, and all of them project to the torus semicircularis (Finger and Tong, 1984; McCormick, 1997; Yamamoto and Ito, 2005). By their shape, the GFP/GLYT2-expressing cells observed in the zebrafish secondary octaval

nucleus might correspond to the spherical cells reported in these teleosts. The ventral fusiform cell population of this nucleus was described as the superior olive in some teleosts, although not in zebrafish.

The medial octavolateral nucleus of the Tg(*glyt2:gfp*) adult zebrafish, the primary mechanoreceptive lateral line center, contains abundant glycinergic cells, including GFP/GLYT2-positive neurons with morphology of crest cells, although apparently lacking dendritic spines. Conspicuous crest cells of the MON with robust dendritic branches (bearing spines?) that extend in the cerebellar crest were GFP-stained in a transgenic zebrafish for *atonal 1a* (Wullimann et al., 2011), although they were probably glutamatergic. Together, these results in the zebrafish medial octavolateral nucleus suggest that different cell types send dendrites branching in the cerebellar crest with a quite similar pattern, i.e. “crest cells” probably represent a heterogeneous population including excitatory (glutamatergic) and inhibitory (glycinergic) cells. It is probable that these cell types have different projections, as suggested by results with other markers in the dorsolateral hindbrain of developing transgenic zebrafish (Sassa et al., 2007). This is similar to the teleost cerebellum where both eurydendroid cells (glutamatergic) and Purkinje cells (GABAergic) send dendrites to the molecular layer but show different axonal projections. The presence of glycinergic and GABAergic crest cells was recently reported in the medial octavolateral nucleus of sturgeon (Adrio et al., 2011). The presence of glycinergic (GFP/GLYT2-positive) populations in the trigeminal descending nuclear complex of zebrafish is not clear excepting its caudal region (medial funicular nucleus). No glycinergic cells were seen in the rodent inferior olive, which is also in agreement with our results in the transgenic zebrafish.

The number of glycinergic (GFP/GLYT2-positive) neurons observed in the gustatory lobes of the facial and vagus nerves of the adult Tg(*glyt2:gfp*) zebrafish is high, which suggests that glycine is widely used in the primary taste centers. This is in contrast with the absence of glycine receptor expression reported by Imboden et al. (2001) in these zebrafish lobes. The presence of glycinergic neurons and fibers was also observed in the facial, glossopharyngeal and vagal viscerosensory lobe of sturgeon (Adrio et al., 2011), although their number was comparatively scant, and in the solitary

complex of rat (Rampon et al., 1996). Very poor GFP-positive fibers were observed in the big secondary gustatory nucleus in the transgenic zebrafish, which receives a prominent secondary gustatory tract from the facial-vagal gustatory lobes, probably indicating that glycinergic cells observed in these taste lobes are local interneurons. This is in contrast with the abundance of glycinergic fibers observed in the secondary gustatory/viscerosensory nucleus of sturgeon (Adrio et al., 2011), putatively arising from glycinergic neurons located in primary viscerosensory centers, which indicate a clear neurochemical difference with zebrafish.

The glycinergic reticulospinal system in zebrafish

Tract-tracing studies in adult zebrafish have revealed a number of neurons in the rhombencephalon projecting to the spinal cord, mostly reticular, raphe, and octavolateral neurons (Lee and Eaton, 1991; Becker et al., 1997). In lampreys, these descending projections are thought to be mostly amino acidergic excitatory (see Buchanan et al., 1987; Brodin et al., 1989), although the existence of reticulospinal neurons with monosynaptic inhibitory glycinergic projections has been recorded (Wannier et al., 1995). Here, retrograde transport from the spinal cord in adult Tg(*glyt2:gfp*) zebrafish revealed the presence of three conspicuous pairs of reticulospinal GFP-positive (and GLYT2 positive) neurons located in the intermediate reticular formation that exhibit differential morphologies. One of these neuron pairs showed long dorsolateral and ventromedial dendrites and contralateral axon. These characteristics correspond with the MiD2cm and MiD3cm cells described in zebrafish and goldfish (Kimmel et al., 1982; Metcalfe et al., 1986; Lee and Eaton, 1991; Lee et al., 1993a; Nakayama and Oda, 2004), which are considered serial homologous of Mauthner cells. This suggests that in zebrafish an accessory Mauthner cell is inhibitory glycinergic. The other two pairs have only ventral or ventrolateral dendrites that appear directed to the ventral or ventrolateral tracts (including possibly the tecto-bulbar tract). These results, together with the thick diameter of their GFP-positive axons, which are neighbor to the MC axon in the medial longitudinal fascicle, suggest that the scarce brain-spinal glycinergic projections observed in zebrafish are highly specialized. The presence of glycinergic reticulospinal cells has also been recently reported in lamprey larvae (Valle-Maroto et al., 2011). Indirect

evidence of the presence of lower brainstem area-spinal cord glycinergic projections has also been obtained in rat using combined wheat germ agglutinin-horseradish peroxidase (WGA-HRP) anterograde transport and glycine immunogold electron microscopy, although the cells of origin of this descending projections were not identified (Holstege and Bongers, 1991).

Glycinergic fibers and the Mauthner cell

The glycinergic synapses on the Mauthner cell of teleosts represent the most studied glycinergic circuit in vertebrates (see Triller et al., 1993; Legendre and Korn, 1994). Here, we showed some adult features of the glycinergic projection on the region of the axon hillock of MC in zebrafish using a Tg(*glyt2:gfp*) transgenic line also used in larval studies of MC innervation (Koyama et al., 2011; Moly and Hatta, 2011). These features include abundance of axon collaterals of a large commissure of thick glycinergic axons derived from a conspicuous group of GFP/GLYT2-positive neurons located at the level of the magnocellular octaval nucleus. This is similar to the report in 4-5 days Tg(*glyt2:gfp*) larvae that most Mauthner cell glycinergic afferents come from contralateral cells (feed-forward glycinergic neurons) located ventrally in the most lateral glycinergic stripe at the level of the MC (Koyama et al., 2011). Other inhibitory afferents come from feedback inhibitory neurons situated in the ventral reticular region (Koyama et al., 2011). Most glycinergic collaterals contact the adult MC around the base of the axon cap, as it has been shown in adult goldfish using glycine immunohistochemistry (Seitanidou et al., 1988; Triller et al., 1993). Comparatively, the number of glycinergic boutons on other parts of the MC is scarce. Other studies have reported a large number of GABAergic boutons contacting the lateral dendrite and cell soma of MC in goldfish (Lee et al., 1993b; Triller et al., 1993) and zebrafish (Castro et al., 2006b). A study in the early Tg(*glyt2:gfp*) zebrafish on contacts of glycinergic axons with the MC reveals that the first glycinergic contacts on this cell arise from ascending axons that contact the lateral part of the soma at 27 hours post-fertilization (Moly and Hatta, 2011). This occurs about the time when first spontaneous glycinergic currents of MC were recorded (Ali et al., 2000). In 42 hours post-fertilization larvae, glycinergic commissural axons contact the anterior and posterior surface of the MC (Moly and Hatta, 2011). At 52 hours post-

fertilization, the zebrafish MC receives morphological and functionally mature glycinergic synapses (Triller et al., 1997). Thus, the prominent projection of glycinergic commissural axons around the MC axon cap shown here must have a comparatively late appearance in development, perhaps by sprouting and specialization of early commissural tracts. Glycinergic projections mediate in adult goldfish strong inhibition in response to vestibular stimulation (see Triller et al., 1993). Rich innervation of the MC by glycinergic axons has also been reported in sturgeon (Adrio et al., 2011), although the richest innervated region of the cell was not the axon hillock but a region of the soma lateral to it.

Glycinergic neurons in the adult spinal cord

The spinal cord contains numerous glycinergic neurons in all studied vertebrates during development (lamprey: Villar-Cerviño et al., 2008b, 2009; zebrafish: Higashijima et al., 2004a,b,c; frog: Dale et al., 1986; Roberts et al., 1988; Wester et al., 2008; chick: Berki et al., 1995; mice: Allain et al., 2006). The distribution of glycinergic neurons of the adult spinal cord was mainly investigated in cat and rodents (see Zeilhofer et al., 2005; Hossaini et al., 2007). However, studies of distribution of glycinergic neurons in adults of non-mammalian vertebrates are scant (lamprey: see Villar-Cerviño et al., 2008b; sturgeon: Adrio et al., 2011; carp: Uematsu et al., 1993). In the spinal cord of developing zebrafish, only a single mediodorsal column of expression of GLYT2 was observed (Higashijima et al., 2004a), and most glycinergic cells pertained to commissural and circumferential subtypes of interneurons (Higashijima et al., 2004b,c; McLean et al., 2007; Liao and Fetcho, 2008). Glycine-ir cells reported in the spinal cord of amphibian embryos are also commissural (Dale et al., 1986; Roberts et al., 1988). Our results in adult Tg(*glyt2:gfp*) transgenic zebrafish indicate that glycinergic (GLYT2/GFP-positive) neurons became diversified in adult fish, showing different populations in association with the medial funicular nucleus (a caudal medullary part of the trigeminal sensory nuclear group; see Xue et al., 2006), dorsal horn, intermediate gray region and ventral horn. This extended distribution of glycinergic neurons is roughly similar to that observed in the adult rat spinal cord with GLYT2 *in situ* hybridization (Hossaini et al., 2007), suggesting a common pattern. The glycinergic populations observed in adult Tg(*glyt2:gfp*) zebrafish are also similar to those reported with glycine

immunohistochemistry in the spinal cord of adult carp (Uematsu et al., 1993). Although correspondence with glycinergic subtypes in larval zebrafish was not investigated, GFP-positive commissural axons were numerous in adult Tg(*glyt2:gfp*) zebrafish. These results in zebrafish suggest involvement of glycinergic cells in various sensory and motor spinal circuits, stressing the importance of glycinergic contralateral inhibition in adult spinal circuits.

LITERATURE CITED

Adrio F, Rodríguez-Moldes I, Anadón R. 2011. Distribution of glycine immunoreactivity in the brain of the Siberian sturgeon (*Acipenser baeri*): comparison with γ-aminobutyric acid. J Comp Neurol 519:1115–1142.

Ali DW, Drapeau P, Legendre P. 2000. Development of spontaneous glycinergic currents in the Mauthner neuron of the zebrafish embryo. J Neurophysiol 84:1726–1736.

Allain AE, Baïri A, Meyrand P, Branchereau P. 2006. Expression of the glycinergic system during the course of embryonic development in the mouse spinal cord and its co-localization with GABA immunoreactivity. J Comp Neurol 496:832–846.

Aprison MH, Werman R. 1965. The distribution of glycine in cat spinal cord and roots. Life Sci 4:2075–2083.

Aprison MH, Daly EC. 1978. Biochemical aspects of transmission in inhibitory synapses: the role of glycine. Adv Neurochem 3:203–294.

Aragón C, López-Corcuera B. 2003. Structure, function and regulation of glycine neurotransporters. Eur J Pharmacol 479:249–262.

Becker T, Wullimann MF, Becker CG, Bernhardt RR, Schachner M. 1997. Axonal regrowth after spinal cord transection in adult zebrafish. J Comp Neurol 377:577–595.

Berki ACS, O'Donovan MJ, Antal M. 1995. Developmental expression of glycine immunoreactivity and its colocalization with GABA in the embryonic chick lumbosacral spinal cord. J Comp Neurol 302:583–596.

Bowery NG, Smart TG. 2006. GABA and glycine as neurotransmitters: a brief history. Br J Pharmacol 147 Suppl 1:S109–119.

Brodin L, Ohta Y, Hökfelt T, Grillner S. 1989. Further evidence for excitatory amino acid transmission in lamprey reticulospinal neurons: selective retrograde labeling with (^{3}H)D-aspartate. J Comp Neurol 281:225–233.

Buchanan JT, Brodin L, Dale N, Grillner S. 1987. Reticulospinal neurones activate excitatory amino acid receptors. Brain Res 408:321–325.

Campistron G, Buijs RM, Geffard M. 1986. Glycine neurons in the brain and spinal cord. Antibody production and immunocytochemical localization. Brain Res 376:400–405.

Castro A, Becerra M, Manso MJ, Anadón R. 2006a. Calretinin immunoreactivity in the brain of the zebrafish, *Danio rerio*: distribution and comparison with some neuropeptides and neurotransmitter-synthesizing enzymes. I. Olfactory organ and forebrain. J Comp Neurol 494:435–459.

Castro A, Becerra M, Manso MJ, Anadón R. 2006b. Calretinin immunoreactivity in the brain of the zebrafish, *Danio rerio*: distribution and comparison with some neuropeptides and neurotransmitter-synthesizing enzymes. II. Midbrain, hindbrain and spinal cord. J Comp Neurol 494:792–814.

Clemente D, Porteros A, Weruaga E, Alonso JR, Arenzana FJ, Aijón J, Arévalo R. 2004. Cholinergic elements in the zebrafish central nervous system: histochemical and immunohistochemical analysis. J Comp Neurol 474:75–107.

Curtis DR, Hösli L, Johnston GA, Johnston IH. 1968. The hyperpolarization of spinal motoneurones by glycine and related amino acids. Exp Brain Res 5:235–258.

Dale N, Ottersen OP, Roberts A, Storm-Mathisen J. 1986. Inhibitory neurones of a motor pattern generator in *Xenopus* revealed by antibodies to glycine. Nature 324:255–257.

Edds-Walton PL, Fay RR, Highstein SM. 1999. Dendritic arbors and central projections of physiologically characterized auditory fibers from the saccule of the toadfish, *Opsanus tau*. J Comp Neurol 411:212–238.

Edds-Walton PL, Holstein GR, Fay RR. 2010. Gamma-aminobutyric acid is a neurotransmitter in the auditory pathway of oyster toadfish, *Opsanus tau*. Hear Res 262:45–55.

Filippi A, Mahler J, Schweitzer J, Driever W. 2010. Expression of the paralogous tyrosine hydroxylase encoding genes th1 and th2 reveals the full complement of dopaminergic and noradrenergic neurons in zebrafish larval and juvenile brain. J Comp Neurol 518:423–438.

Finger TE, Tong SL. 1984. Central organization of eighth nerve and mechanosensory lateral line system in the catfish: *Ictalurus nebulosus*. J Comp Neurol 229:129–151.

Guastella J, Brecha N, Weigmann C, Lester HA, Davidson N. 1992. Cloning, expression, and localization of a rat brain high-affinity glycine transporter. Proc Natl Acad Sci USA 89:7189–7193.

Higashijima S, Mandel G, Fetcho JR. 2004a. Distribution of prospective glutamatergic, glycinergic, and GABAergic neurons in embryonic and larval zebrafish. J Comp Neurol 480:1–18.

Higashijima S, Schaefer M, Fetcho JR. 2004b. Neurotransmitter properties of spinal interneurons in embryonic and larval zebrafish. J Comp Neurol 480:19–37.

Higashijima S, Masino MA, Mandel G, Fetcho JR. 2004c. Engrailed-1 expression marks a primitive class of inhibitory spinal interneuron. J Neurosci 24:5827–5839.

Holstege JC, Bongers CM. 1991. A glycinergic projection from the ventromedial lower brainstem to spinal motoneurons. An ultrastructural double labeling study in rat. Brain Res 566:308–315.

Hossaini M, French PJ, Holstege JC. 2007. Distribution of glycinergic neuronal somata in the rat spinal cord. Brain Res 1142:61–69.

Hunter PR, Nikolaou N, Odermatt B, Williams PR, Drescher U, Meyer MP. 2011. Localization of Cadm2a and Cadm3 proteins during development of the zebrafish nervous system. J Comp Neurol 519:2252-2270.

Imboden M, Devignot V, Korn H, Goblet C. 2001. Regional distribution of glycine receptor messenger RNA in the central nervous system of zebrafish. Neuroscience 103:811–830.

Johnson JW, Ascher P. 1987. Glycine potentiates the NMDA response in cultured mouse brain neurons. Nature 325:529–531.

Kaslin J, Panula P. 2001. Comparative anatomy of the histaminergic and other aminergic systems in zebrafish (*Danio rerio*). J Comp Neurol 440:342–777.

Kimmel CB, Powell SL, Metcalfe WK. 1982. Brain neurons which project to the spinal cord in young larvae of the zebrafish. J Comp Neurol 205:112–127.

Kinkhabwala A, Riley M, Koyama M, Monen J, Satou C, Kimura Y, Higashijima S, Fetcho J. 2011. A structural and functional ground plan for neurons in the hindbrain of zebrafish. Proc Natl Acad Sci U S A 108:1164–1169.

Koyama M, Kinkhabwala A, Satou C, Higashijima S, Fetcho J. 2011. Mapping a sensory-motor network onto a structural and functional ground plan in the hindbrain. Proc Natl Acad Sci U S A 108:1170–1175.

Kuscha V, Barreiro-Iglesias A, Becker CG, Becker T. 2012. Plasticity of tyrosine hydroxylase and serotonergic systems in the regenerating spinal cord of adult zebrafish. J Comp Neurol 520:933-951.

Landwehr S, Dicke U. 2005. Distribution of GABA, glycine, and glutamate in neurons of the medulla oblongata and their projections to the midbrain tectum in plethodontid salamanders. J Comp Neurol 490:145–162.

Lannoo MJ, Hawkes R. 1997. A search for primitive Purkinje cells: zebrin II expression in sea lampreys (*Petromyzon marinus*). Neurosci Lett 237:53–55.

Lee RKK, Eaton RC. 1991. Identifiable reticulospinal neurons of the adult zebrafish, *Brachydanio rerio*. J Comp Neurol 304:34–52.

Lee RKK, Eaton RC, Zottoli SJ. 1993a. Segmental arrangement of reticulospinal neurons in the goldfish hindbrain. J Comp Neurol 329:539–556.

Lee RKK, Finger TE, Eaton RC. 1993b. GABAergic innervation of the Mauthner cell and other reticulospinal neurons in the goldfish. J Comp Neurol 338:601–611.

Legendre P, Korn H. 1994. Glycinergic inhibitory synaptic currents and related receptor channels in the zebrafish brain. Eur J Neurosci 6:1544-1557.

Liao JC, Fetcho JR. 2008. Shared versus specialized glycinergic spinal interneurons in axial motor circuits of larval zebrafish. J Neurosci 28:12982-12192.

Lieberoth BC, Becker CG, Becker T. 2003. Double labeling of neurons by retrograde axonal tracing and non-radioactive in situ hybridization in the CNS of adult zebrafish. Methods Cell Sci 25:65–70.

Liu QR, Mandiyan S, Nelson H, Nelson N. 1992. A family of genes encoding neurotransmitter transporters. Proc Nat1 Acad Sci USA 89: 6639–6643.

Liu QR, López-Corcuera B, Mandiyan S, Nelson H, Nelson N. 1993. Cloning and expression of a spinal cord- and brain-specific glycine transporter with novel structure features. J Biol Chem 268:22802–22808.

Ma PM. 1997. Catecholaminergic systems in the zebrafish. III. Organization and projection pattern of medullary dopaminergic and noradrenergic neurons. J Comp Neurol 381:411-427.

McCormick CA. 1997. Organization and connections of octaval and lateral line centers in the medulla of a clupeid, *Dorosoma cepedianum*. Hear Res 110:39–60.

McCormick CA, Braford MR Jr. 1988. Central connections of the octavolateralis system: evolutionary considerations. In: Atema J, Fay RR, Popper AN, Tavolga WN (Editors), Sensory Biology of Aquatic Animals. New York: Springer-Verlag, p. 341–364.

McLean DL, Fan J, Higashijima S, Hale ME, Fetcho JR. 2007. A topographic map of recruitment in spinal cord. Nature 446:71–75.

Meng S, Ryu S, Zhao B, Zhang DQ, Driever W, McMahon DG. 2008. Targeting retinal dopaminergic neurons in tyrosine hydroxylase-driven green fluorescent protein transgenic zebrafish. Mol Vis 14:2475-2483.

Metcalfe WK, Mendelson B, Kimmel CB. 1986. Segmental homologies among reticulospinal neurons in the hindbrain of the zebrafish larva. J Comp Neurol 251:147–159.

Moly PK, Hatta K. 2011. Early glycinergic axon contact with the Mauthner neuron during zebrafish development. Neurosci Res 70:251–259.

Mueller T, Guo S. 2009. The distribution of GAD67-mRNA in the adult zebrafish (teleost) forebrain reveals a prosomeric pattern and suggests

previously unidentified homologies to tetrapods. J Comp Neurol 516:553–568.

Mueller T, Vernier P, Wullimann MF. 2004. The adult central nervous cholinergic system of a neurogenetic model animal, the zebrafish *Danio rerio*. Brain Res 1011:156–169.

Mueller T, Vernier P, Wullimann MF. 2006. A phylotypic stage in vertebrate brain development: GABA cell patterns in zebrafish compared with mouse. J Comp Neurol 494:620–634.

Nakayama H, Oda Y. 2004. Common sensory inputs and differential excitability of segmentally homologous reticulospinal neurons in the hindbrain. J Neurosci 24:3199–3209.

O'Donovan M, Sernagor E, Sholomenko G, Ho S, Antal M, Yee W. 1992. Development of spinal motor networks in the chick embryo. J Exp Zool 261:261–273.

Parsons CG, Danysz W, Hesselink M, Hartmann S, Lorenz B, Wollenburg C, Quack G. 1998. Modulation of NMDA receptors by glycine--introduction to some basic aspects and recent developments. Amino Acids 14:207–216.

Pierce LX, Noche RR, Ponomareva O, Chang C, Liang JO. 2008. Novel functions for Period 3 and Exo-rhodopsin in rhythmic transcription and melatonin biosynthesis within the zebrafish pineal organ. Brain Res 1223:11-24.

Poyatos I, Ponce J, Aragón C, Giménez C, Zafra F. 1997. The glycine transporter GLYT2 is a reliable marker for glycine-immunoreactive neurons. Mol Brain Res 49:63–70.

Pourcho RG, Goebel DJ, Jojich L, Hazlett JC. 1992. Immunocytochemical evidence for the involvement of glycine in sensory centers of the rat brain. Neuroscience 46:643–656.

Rampon C, Luppi PH, Fort P, Peyron C, Jouvet M. 1996. Distribution of glycine-immunoreactive cell bodies and fibers in the rat brain. Neuroscience 75:737–755.

Redecker P, Pabst H, Löscher W, Steinlechner S. 2001. Evidence for microvesicular storage and release of glycine in rodent pinealocytes. Neurosci Lett 299:93–96.

Reichenberger I, Streit P, Ottersen OP, Dieringer N. 1993. GABA- and glycine-like immunoreactivities in the cerebellum of the frog. Neurosci Lett 154:89–92.

Reichenberger I, Straka H, Ottersen OP, Streit P, Gerrits NM, Dieringer N. 1997. Distribution of GABA, glycine, and glutamate immunoreactivities in the vestibular nuclear complex of the frog. J Comp Neurol 377:149–164.

Roberts A, Dale N, Ottersen OP, Storm-Mathisen J. 1988. Development and characterization of commissural interneurones in the spinal cord of *Xenopus laevis* embryos revealed by antibodies to glycine. Development 103:447–461.

Rovsing L, Clokie S, Bustos DM, Rohde K, Coon SL, Litman T, Rath MF, Møller M, Klein DC. 2011. Crx broadly modulates the pineal transcriptome. J Neurochem 119:262-274.

Saint Marie RL, Ostapoff EM, Morest DK, Wenthold RJ. 1989. Glycine-immunoreactive projection of the cat lateral superior olive: possible role in midbrain ear dominance. J Comp Neurol 279:382-396.

Sassa T, Aizawa H, Okamoto H. 2007. Visualization of two distinct classes of neurons by gad2 and zic1 promoter/enhancer elements in the dorsal hindbrain of developing zebrafish reveals neuronal connectivity related to the auditory and lateral line systems. Dev Dyn 236:706–718.

Sato K, Kiyama H, Shimada S, Tohyama M. 1993. Gene expression of KA type and NMDA receptors and of a glycine transporter in the rat pineal gland. Neuroendocrinology 58:77–99.

Seitanidou T, Triller A, Korn H. 1988. Distribution of glycine receptors on the membrane of a central neuron: an immunoelectron microscopy study. J Neurosci 8:4319–4333.

Smith KE, Borden LA, Hatting PR, Branchek T, Weinshank RL. 1992. Cloning and expression of a glycine transporter reveal co-localization with NMDA receptors. Neuron 8927–8935.

Tanaka I, Ezure K. 2004. Overall distribution of GLYT2 mRNA-containing versus GAD67 mRNA-containing neurons and colocalization of both mRNAs in midbrain, pons, and cerebellum in rats. Neurosci Res 49:165-178.

Tanaka I, Ezure K, Kondo M. 2003. Distribution of glycine transporter 2 mRNA-containing neurons in relation to glutamic acid decarboxylase mRNA-containing neurons in rat medulla. Neurosci Res 47:139-151.

Triller A, Sur C, Korn H. 1993. Heterogeneous distribution of glycinergic and GABAergic afferents on an identified central neuron. J Comp Neurol 338:83–96.

Triller A, Rostaing P, Korn H, Legendre P. 1997. Morphofunctional evidence for mature synaptic contacts on the Mauthner cell of 52-hour-old zebrafish larvae. Neuroscience 80:133–145.

Uematsu K, Shirasaki M, Storm-Mathisen J. 1993. GABA- and glycine-immunoreactive neurons in the spinal cord of the carp, *Cyprinus carpio*. J Comp Neurol 332:59–68.

Valle-Maroto SM, Fernández-López B, Villar-Cerviño V, Barreiro-Iglesias A, Anadón R, Rodicio MC. 2011. Inhibitory descending rhombencephalic projections in larval sea lamprey. Neuroscience 194:1–10.

Van den Pol AN, Gorcs T. 1988. Glycine and glycine receptor immunoreactivity in brain and spinal cord. J Neurosci 8: 472–492.

Vatine G, Vallone D, Appelbaum L, Mracek P, Ben-Moshe Z, Lahiri K, Gothilf Y, Foulkes NS. 2009. Light directs zebrafish period2 expression via conserved D and E boxes. PLoS Biol 7(10):e1000223.

Villar-Cerviño V, Barreiro-Iglesias A, Anadón R, Rodicio MC. 2008a. Distribution of glycine immunoreactivity in the brain of adult sea lamprey (*Petromyzon marinus*). Comparison with gamma-aminobutyric acid. J Comp Neurol 507:1441–1463.

Villar-Cerviño V, Holstein GR, Martinelli GP, Anadón R, Rodicio MC. 2008b. Glycine-immunoreactive neurons in the developing spinal cord of the sea lamprey: comparison with the gamma-aminobutyric acidergic system. J Comp Neurol 508:112–130.

Villar-Cerviño V, Barreiro-Iglesias A, Anadón R, Rodicio MC. 2009. Development of glycine immunoreactivity in the brain of the sea lamprey: comparison with gamma-aminobutyric acid immunoreactivity. J Comp Neurol 512:747–767.

Walberg F, Ottersen OP, Rinvik E. 1990. GABA, glycine, aspartate, glutamate and taurine in the vestibular nuclei: an immunocytochemical investigation in the cat. Exp Brain Res 79:547–563.

Wannier T, Orlovsky G, Grillner S. 1995. Reticulospinal neurones provide monosynaptic glycinergic inhibition of spinal neurones in lamprey. Neuroreport 6:1597–1600.

Wenthold RJ, Huie D, Altschuler RA, Reeks KA. 1987. Glycine immunoreactivity localized in the cochlear nucleus and superior olivary complex. Neuroscience 22:897–912.

Wester MR, Teasley DC, Byers SL, Saha MS. 2008. Expression patterns of glycine transporters (*xGlyT1*, *xGlyT2*, and *xVIAAT*) in *Xenopus laevis* during early development. Gene Expr Patterns 8:261–270.

Westerfield M. 1989. The zebrafish book: a guide for the laboratory use of zebrafish (*Brachydanio rerio*). Eugene: University of Oregon Press.

Wullimann MF, Rupp B, Reichert H. 1996. Neuroanatomy of the zebrafish brain. A topological atlas. Basel: Birkhäuser.

Wullimann MF, Mueller T, Distel M, Babaryka A, Grothe B, Köster RW. 2011. The long adventurous journey of rhombic lip cells in jawed vertebrates: a comparative developmental analysis. Front Neuroanat Apr 21;5:27.

Xue HG, Yang CY, Ito H, Yamamoto N, Ozawa H. 2006. Primary and secondary sensory trigeminal projections in a cyprinid teleost, carp (*Cyprinus carpio*). J Comp Neurol 499:626–644.

Yamamoto K, Ruuskanen JO, Wullimann MF, Vernier P. 2010 Two tyrosine hydroxylase genes in vertebrates. New dopaminergic territories revealed in the zebrafish brain. Mol Cell Neurosci 43:394–402.

Yamamoto N, Ito H. 2005. Fiber connections of the central nucleus of semicircular torus in cyprinids. J Comp Neurol 491:186–211.

Yáñez J, Busch J, Anadón R, Meissl H. 2009. Pineal projections in the zebrafish (*Danio rerio*): overlap with retinal and cerebellar projections. Neuroscience 164:1712-1720.

Yang CY, Yoshimoto M, Xue HG, Yamamoto N, Imura K, Sawai N, Ishikawa Y, Ito H. 2004. Fiber connections of the lateral valvular nucleus in a

percomorph teleost, tilapia (*Oreochromis niloticus*). J Comp Neurol 474:209–226.

Young AB, Snyder SH. 1974. The glycine synaptic receptor: evidence that strychnine binding is associated with the ionic conductance mechanism. Proc Natl Acad Sci U S A 71:4002–4005.

Zafra F, Gomeza J, Olivares L, Aragón C, Giménez C. 1995a. Regional distribution and developmental variation of the glycine transporters GLYT1 and GLYT2 in the rat CNS. Eur J Neurosci 7:1342–1352.

Zafra F, Aragón C, Olivares L, Danbolt NC, Giménez C, Storm-Mathisen J. 1995b. Glycine transporters are differentially expressed among CNS cells. J Neurosci 15:3952–3969.

Zeilhofer HU, Studler B, Arabadzisz D, Schweizer C, Ahmadi S, Layh B, Bosl MR, Fritschy JM. 2005. Glycinergic neurons expressing enhanced green fluorescent protein in bacterial artificial chromosome transgenic mice. J Comp Neurol 482:123–141.

FIGURE LEGENDS

Figure 1. Schematic drawings of transverse sections of the adult Tg(*glyt2:gfp*) zebrafish brain showing the main anatomical structures in the left side. The distribution of populations showing GFP-positive/GLYT2-positive perikarya (large black dots), GLYT2-positive/GFP-negative (lozenges, in pink in the online version) and GFP-positive-GLYT2-negative neurons (triangles, in green in the online version) is shown in the right side of sections. GFP-positive fibers (dashes) are also represented in the right side. In levels J-L, the periventricular cell layer of the torus semicircularis is represented by the gray-shaded region on the left side. The schematic profiles of the three characteristic pairs of glycinergic reticulospinal neurons and their descending axons are also drawn on the left side of levels P-X (in red in the online version). The GFP-negative Mauthner cell is drawn on the left in level O and the Mauthner axon (arising from the contralateral MC) is also indicated in levels P-X (in blue in the online version). In the cerebellar crest (levels O-R), some GFP-positive crest cell dendrites are depicted. The levels of sections are indicated by lines in the

figures representing a lateral view of the brain. Asterisks indicate ventricular cavities. For abbreviations, see list. Scale bars: 200 µm.

Figure 2. Photomicrographs of representative sections of the zebrafish brain showing perikarya expressing GLYT2 mRNA, ordered from rostral (A) to caudal (J). **A**, GLYT2-positive neurons are observed in a small group of the midbrain tegmentum (black arrow). **B-J**, Numerous GLYT2-positive cells were distributed throughout most regions of the rhombencephalon. Note the large differences in staining intensity among neuronal populations. For abbreviations, see list. Black arrow in D points to the dorsal cell cluster caudal to the dorsal trigeminal motor nucleus. Outlined arrows in A and F indicate the oculomotor and octaval nerve, respectively. Approximate correspondence with levels in drawings of Figure 1 is indicated in the upper right corner. Scale bars = 100 µm.

Figure 3. Confocal photomicrographs of representative populations of the octavolateral region showing partial colocalization of GFP-immunofluorescence (green channel, left) and GLYT2 mRNA *in situ* hybridization (magenta channel, central) in the right panels (merged channels). **A-C**, Medial octavolateral nucleus showing two types of positive neurons. Small cells (arrowheads) show clear colocalization but strong GLYT2 reaction in crest cells (double arowhead) obscured GFP immunofluorescence, although it is visible in the apical dendrite of the pointed cell. Note also GFP-positive/GLYT2 negative cells (arrow). **D-F**, Glycinergic nucleus at the level of the magnocellular octaval nucleus showing GLYT2/GFP double labeled cells (arrowheads). **G-I**, Tangential nucleus exhibiting GLYT2-positive but GFP-negative cells (outlined arrow). **J-L**, Secondary octaval nucleus exhibiting double positive neurons, some indicated by arrowheads. Scale bars: 20 µm.

Figure 4. Confocal photomicrographs of representative rhombencephalic glycinergic populations showing partial colocalization of GFP-immunofluorescence (green channel, left) and GLYT2 mRNA *in situ* hybridization product (magenta channel, central) in the right panels (merged channels). **A-C**, Section of the facial lobe showing faint GLYT2 staining in a

part of the GFP-positive cells (arrowheads). Note also GFP-positive/GLYT2 negative cells (arrow). **D-F**, Section of the intermediate reticular formation. Arrowheads point to some cells showing clearly GFP /GLYT2 colocalization, the arrow to a GFP-positive/GLYT2-negative cell. **G-I**, Large GFP-positive reticular cell (arrowhead) showing moderate GLYT2 expression. This cell corresponds to the spinal-projecting glycinergic cells shown in figure 11F. Scale bars: 20 µm.

Figure 5. Sections of the adult Tg(*glyt2:gfp*) zebrafish forebrain showing GFP-expressing cells (A-E), and GFP expression in fibers of the olfactory bulb (F) and telencephalon (G-H). **A**, Transverse section of the ventral hypothalamus showing a group of small cells (arrow) below the anterior tuberal nucleus. **B**, Transverse section of the diencephalon passing through the medial preglomerular nucleus showing a group of medium-sized GFP-positive cells (arrow). **C**, Transverse section of the caudal diencephalon showing scattered small GFP-positive cells lateral to the posterior commissure (arrows). Note also a band of GFP-positive fibers in the zona limitans and ascending fibers densely innervating the pretectal area. **D-E**, Sagittal section passing through the pineal organ showing the large population of small GFP-positive cells. In E, note processes of these cells coursing to a basal neuropil in the neuroepithelium (outlined arrow). **F**, Sagittal section showing GFP-positive fibers scattered through the olfactory bulb, mainly in inner regions. Arrowheads point to olfactory glomeruli. Rostral is at the right. **G**, Transverse section showing the scarcity of GFP-positive fibers in the dorsal telencephalic area (pallium). **H**, Transverse section at the level of the anterior commissure showing GFP-positive fibers coursing mostly laterally to it. Angled arrows in A, G and H point to autofluorescent blood vessels. A,D-H, GFP fluorescence; B-C, GFP immunofluorescence. For abbreviations, see list. Scale bars: 50 µm (A-D, F-H), 10 µm (E).

Figure 6. Confocal photomicrographs of transverse sections through the diencephalon and optic tectum of the adult Tg(*glyt2:gfp*) zebrafish. **A**, Section at the level of the suprachiasmatic nucleus showing the crossing of GFP-positive fibers in the postoptic commissure. **B**, Section though the superficial

pretectum showing the rich GFP-positive innervation of the magnocellular nucleus. **C**, Section at a lateral level of the pretoral region showing the entrance of thick GFP-positive fibers to the optic tectum. **D**, Section through the rostral optic tectum showing thick GFP-positive fibers in the stratum album centrale and thinner fibers in other strata. **E**, Detail of plexuses of GFP-positive fibers in the layers of the optic tectum. **F-H**, Photomicrographs of the nucleus of the medial longitudinal fascicle showing in F the GFP-positive fibers (green), in G the large cells retrogradely labeled from the spinal cord (in magenta) and in H the merged channels. **I**, Section passing through the rostral midbrain tegmentum showing scarce GFP-positive fibers in the red nucleus, which shows cells retrogradely labeled from the spinal cord (arrowed, in color in the digital edition). For abbreviations, see list. A, GFP immunofluorescence; B-I, GFP fluorescence (alone or combined with biocytin detection). In B, C, D and E, medial is at the right; in F-I, the midline is indicated by vertical dashes. Scale bars: 50 µm (A-C, E-I), 100 µm (D).

Figure 7. Confocal photomicrographs of transverse (A-C) and parasagittal (D-F) sections through the mesencephalic tegmentum of the adult Tg(*glyt2:gfp*) zebrafish showing the distribution of GFP-expressing cells and fibers. **A** and **D**, Sections at the level of the medial fiber plexus of the torus semicircularis/midbrain lateral reticular region (outlined arrows and asterisks, respectively) and the GFP-expressing small cells located in the medial region of the central nucleus of the torus (arrows). Inset in A, detail of the cells. **B-C** and **E-F**, Sections showing the dense plexus of glycinergic fibers in the midbrain lateral reticular region (asterisks). Note also thick glycinergic fibers ascending in the lateral longitudinal fascicle toward the pretectum and tectum. In A-C, midline is indicated by vertical dashes. In D-F, rostral is at the right. For abbreviations, see list. All figures are of GFP fluorescence except the inset in figure A, which was revealed by GFP immunofluorescence. For the anatomical location of the GFP-positive cell containing region in Nissl-stained sections, see Figure 8. Scale bars: 100 µm (A-C, E-F), 50 µm (D), 25 µm (inset in A).

Figure 8. Nissl-staining (A) and GFP fluorescence (B) in transverse sections of adult zebrafish passing through the region of the central nucleus of the torus semicircularis showing the location of the region containing GFP-positive cells with respect to the TSc periventricular layer and other nuclei and structures. Thick outlined arrows indicate the same region in both sections (Figure in color in the online version). The thin arrows point to the ventricular sulcus separating the torus and the lateral nucleus of the valvula. A, light microscopy, wild type zebrafish. B, confocal fluorescence and background microscopy, transgenic zebrafish. For abbreviations, see list. Scale bars, 50 µm.

Figure 9. **A-F**, Confocal photomicrographs of transverse sections through the octavolateral region of adult Tg(*glyt2:gfp*) zebrafish showing the distribution of GFP-positive neurons (green) and their topographical relationship to spinal projecting neurons of this region (in magenta). In E, small arrow points to a small spinal-projecting cell. **G**, Detail of GFP-positive crest cells of the medial octavolateral nucleus sending long dendrites to the cerebellar crest. Note also small glycinergic cells in this nucleus. **H**, Detail of GFP-positive cells in the octavolateral nuclei (MON, AON and MaON) at the level of the octaval nerve entrance. Retrogradely labeled octaval cells are shown in magenta. **I**, Detail of the large GPF-positive neurons of the secondary octaval nucleus and the rich terminal field. Outlined arrows in D-E and G point to GFP-positive fibers crossing in a dorsal commissure joining secondarily the octavolateral nuclei of both sides. In A, C, E, F, midline is indicated by vertical dashes. In other panels, medial is at the right. For abbreviations see list. Scale bars: 100 µm (A-F), 50 µm (D), 25 µm (H, I).

Figure 10. **A-C**, Confocal photomicrographs showing the distribution of GFP-expressing neurons in transverse sections of the medulla of adult Tg(*glyt2:gfp*) zebrafish at the level of the facial lobe (A), vagal lobe (B) and commissural nucleus (C). Outlined arrowheads point to glycinergic reticular neurons. **D**, Detail showing the appearance of small glycinergic neurons of the facial lobe. **E**, Detail showing the neurons of the vagal lobe and the superficial layer of

glycinergic fibers (arrows). In A-D, vertical dashes indicate the midline. For abbreviations, see list. Scale bars: 100 µm (A-C), 20 µm (D-E).

Figure 11. Confocal photomicrographs of transverse sections through the rhombencephalon of the adult Tg(*glyt2:gfp*) zebrafish arranged rostrocaudally showing GFP-expressing structures in green, and cells and fibers labeled from the spinal cord in magenta. Double-labeled cells appear in white. **A-B**, Sections showing the most rostral rhombencephalic glycinergic cells located ventrally to the large reticulospinal neurons of the superior reticular nucleus. A small dorsal cluster of GFP-positive neurons (arrowhead) is shown caudally to the dorsal trigeminal motor nucleus (not appearing at this level). **C**, Section at the level of the Mauthner cells showing abundant glycinergic neurons in the intermediate reticular nucleus. Note the conspicuous GFP-positive commissural fibers at the level of Mauthner cells. **D**, Section showing the rostral pair of GFP-positive reticulospinal neurons (arrow) located caudally to the Mauthner cell (photomontage of two adjacent sections). Note the ventrolateral dendrite (arrowhead). **E**, Section showing the second pair of glycinergic reticulospinal neurons (arrow). These cells with contralateral axons correspond to the accessory Mauthner cell. Note long dorsal (double arrowhead) and ventral (arrowhead) dendrites of these cells and the exit of axons (outlined arrowhead). Angled arrow points to a double-labeled small cell close to a large glycinergic reticulospinal cell. Photomontage of three adjacent sections. **F**, Section at a level just rostral to the facial lobe showing the third pair of large reticulospinal glycinergic neurons (arrow). Note the thick branched ventral dendrite (arrowhead) and the initial segment of the axon (outlined arrowhead). **G-I**, Sections showing GFP-positive neurons in the inferior reticular nucleus at the level of the facial lobe (G-H) and vagal lobe (I). In G, note a retrogradely labeled glycinergic neuron in the raphe nucleus (arrow). Asterisks in E-I indicate the Mauthner axon. In E-I, note also thick axons of retrogradely labeled GFP-positive cells in the dorsal part of the medial longitudinal fascicle. Outlined arrow in I points to a conspicuous ventrolateral fascicle of glycinergic fibers coursing in the caudal medulla and spinal cord. Vertical dashes indicate the midline. For abbreviations, see list. Scale bars: 100 µm (A-I).

Figure 12. Confocal photomicrographs of transverse (A-G) and oblique sagittal sections of the rhombencephalon of adult Tg(*glyt2:gfp*) zebrafish showing the glycinergic innervation of the Mauthner cell (MC). Glycinergic structures appear in green and retrogradely labeled cells in magenta. **A**, Section passing through the commissure of thick glycinergic fibers (thick arrow) at the level of retrogradely labeled Mauthner neurons. The outlined arrow points to the ventral dendrite of MC. **B**, Section passing through the labeled MC cell body (arrowhead) at the level of the axon exit, which is surrounded by numerous glycinergic fibers. Note also the compact group of glycinergic cells (double arrow) laterally to MC and the Mauthner axon (angled arrow). **C**, Section passing through the MC axon (angled arrow). The outlined arrow points to the ventral dendrite and the thick arrow points to the commissural fibers. **D**, Section showing the branching of the ventral dendrite (outlined arrow) of a retrogradely labeled MC. The white arrow points to glycinergic commissural fibers. **E-F**, Detail of the thick ventral MC dendrite (outlined arrow) showing scarce glycinergic innervation. E, merged channels, E', glycinergic fibers. **G-H**, Detail of the thick ventral dendrite (outlined arrow) showing rather scarce glycinergic innervation. F, merged channels, F', glycinergic fibers. Inset, detail of the small glycinergic boutons around the MC dendrite. **I**, Transverse section at the level of the dorsal glycinergic commissure showing numerous thin collaterals of thick fibers that contact the region of the MC perikaryon (white arrowhead) around the axon hillock indicated by thin white arrows. Outlined arrowheads indicate branching fibers. The outlined thick arrow points to the axon cap. **J, K**, Details of two confocal planes of a sagittal section passing through the axon cap (indicated by the outlined arrow) of the MC (unlabeled) at proximal (J) and more distal (K) levels showing thin collaterals of the thick commissural glycinergic fibers embracing the axon hillock region. Double arrows point to glycinergic neurons, the asterisk indicates a glycine-negative dorsal commissural tract. Inset in J shows a detail of the branching of the glycinergic fiber pointed by an arrowhead. In A and D, vertical dashes indicate the midline. In B-C and E-I, medial is at the right. In J-K, rostral is at the right. For abbreviation, see list. Scale bars: 100 µm (A), 50 µm (B, C, D, G-H, J, K), 30 µm (inset in H), 25 µm (E-F, I, inset in J).

Figure 13. **A-D**, Transverse sections through the caudal medulla and rostral spinal cord from more rostral (A) to more caudal (D) showing the distribution of GFP-positive cells and fibers in adult Tg(*glyt2:gfp*) zebrafish. Note the different cells size of dorsal and ventral horn cells, and the abundance of glycinergic processes in the ventral horn and ventrolateral funiculus. Thin arrows point to ventral horn medium-sized glycinergic neurons. Outlined arrows point to thick glycinergic axons coursing in the dorsal part of the mlf. Arrowheads point to commissural fibers crossing between the dorsal and ventral parts of the mlf. Asterisks indicate the location of MC giant axons. Angled arrows point to a ventrolateral tract of thick glycinergic axons. For abbreviations, see list. Scale bars: 100 µm (A, B, C, D).

Figure 14. Confocal photomicrographs of transverse sections of adult wild type zebrafish brain showing glycine immunofluorescence in neurons (in E-F) and fibers. **A**, Section showing glycine-ir fibers in the olfactory bulb. Outlined arrowheads point to blood vessels. **B**, Section of the caudal telencephalon showing scarce glycine-ir fibers. The arrow points to fibers shown in the inset. Outlined arrowheads, blood vessels. **C**, Transition between the pretectum and rostral optic tectum showing glycine-ir fibers passing to the tectum (arrow). Outlined arrowhead, blood vessel. **D**, Optic tectum showing the stratified distribution of glycine-ir fibers. The arrow points to fibers shown in the inset. Outlined arrowheads, blood vessels. **E**, Torus semicircularis at the level of the small-celled glycinergic population (arrow). Inset, detail of these glycine-ir cells. Outlined arrowheads, blood vessels. **F**, Medial octavolateral nucleus showing larger cells with dendrites extending in the cerebellar crest (arrow) and small cells. Vertical bars indicate the midline (A, B, F). In C, D and E, medial is at the right. For abbreviations, see list. Correspondence with levels in Figure 1 is indicated. Magnification of insets is double than in corresponding figures. Scale bars, 50 µm (A, C, D, E, F), 100 µm (B).

Figure 15. Confocal photomicrographs of transverse sections of adult wild type zebrafish brain showing glycine immunofluorescence in neurons and fibers. **A**, Alar rhombencephalon showing glycine-ir cells in the descending octaval nucleus and lateral to the trigeminal descending tract (arrow). Inset, detail of

arrowed cells. **B**, Secondary octaval nucleus showing glycine-ir neurons (arrow). Inset, detail of arrowed cells. Outlined arrowhead, blood vessel. **C**, Section through the facial and vagal lobes showing small glycine-ir cells. Inset, detail of the arrowed cells. Outlined arrowhead, blood vessel. **D**, Section showing glycine-ir cells in the inferior reticular formation. The arrowed small cells are magnified in the inset. The outlined arrow points to a larger reticular neuron. Outlined arrowhead, blood vessel. **E**, Section through the caudal medulla showing glycine-ir cells in the medial funicular nucleus (arrow). Inset, detail of arrowed cells. **F**, Section of the spinal cord showing glycine-ir cells of the ventral horn (arrows). Inset, detail of the solid arrow-pointed cells. Vertical bars indicate the midline (A-F). For abbreviations, see list. Correspondence with levels in Figure 1 is indicated. Magnification of insets is double than in corresponding figures. Scale bars, 50 µm (A, B, F), 100 µm (C, D, E).

Abbreviations

1	rostral pair of glycinergic reticulospinal cells
2	intermediate pair of glycinergic reticulospinal cells (M' cell?)
3	caudal pair of glycinergic reticulospinal cells
ac	anterior commissure
an	ansulate commissure
AON	anterior octaval nucleus
AP	area postrema
APN	accessory pretectal nucleus
AT	anterior thalamic nucleus
ATN	anterior tuberal nucleus
CB	cerebellar body
CC	cerebellar crest
CG	rhombencephalic central gray
CIL	central nucleus of the inferior hypothalamic lobe
CN	commissural nucleus (of Cajal)
CON	caudal octaval nucleus
CP	central posterior thalamic nucleus
ca	central canal

csp commissure of superficial pretectum
ctg commissural fibers of octaval tangential nucleus
cven ventral commissure
D dorsal telencephalon (pallium)
DAO dorsal accessory optic nucleus
Dc central zone of dorsal telencephalon
Dd dorsal zone of dorsal telencephalon
DH dorsal horn of spinal cord
Dl lateral zone of dorsal telencephalon
Dla anterior part of Dl
Dm medial part of dorsal telencephalon
Dma anterior part of Dm
DON descending octaval nucleus
DP dorsal posterior thalamic nucleus
Dp posterior zone of dorsal telencephalon
dV trigeminal descending root
EG granular eminence of cerebellum
En entopeduncular nucleus
fr fasciculus retroflexus
Gl glomerular layer
glyc glycinergic commissure at the level of Mauthner cells
gn glycinergic neuropil of TSc
GR granular layer
H habenula
hc horizontal commissure
Hy hypophysis
HY hypothalamus
HYc caudal hypothalamus
HYv ventral hypothalamus
IIIN oculomotor nucleus
IIIv third ventricle
IMR intermediate reticular formation
IO inferior olive
IP interpeduncular nucleus

IR inferior reticular formation

IVN trochlear nucleus

IX glossopharyngeal nerve

lfb lateral forebrain bundle

LFN lateral funicular nucleus

LIX glossopharyngeal lobe

ll lateral longitudinal fascicle (lateral lemniscus)

lot lateral olfactory tract

LR lateral hypothalamic recess

LVII facial lobe

LX vagal lobe

MaON magnocellular octaval nucleus

MC Mauthner cell

mfb medial forebrain bundle

MFN medial funicular nucleus

ML molecular layer

mlf medial longitudinal fascicle

MON medial octavolateral nucleus

MPo magnocellular preoptic nucleus

MT mesencephalic tegmentum

NDLI diffuse nucleus of the inferior hypothalamic lobe

NI isthmic nucleus

NLV lateral nucleus of the valvula

Nmlf nucleus of the medial longitudinal fascicle

OB olfactory bulb

OC optic chiasm

ON optic nerve

OT optic tectum

otr optic tract

OVLT vascular organ of the terminal lamina

P pineal organ

PA pretectal area

pc posterior commissure

PGa anterior preglomerular nucleus

PGl lateral preglomerular nucleus
PGm medial preglomerular nucleus
PL perilemniscular nucleus
PO posterior thalamic nucleus
POA preoptic area
poc postoptic commissure
Ppa parvocellular preoptic nucleus, anterior part
Ppp parvocellular preoptic nucleus, posterior part
Ppt periventricular pretectum
PT pretectum
PTN posterior tuberal nucleus
PSM magnocellular superficial pretectal nucleus
PSP parvocellular superficial pretectal nucleus
PTO pretoral nucleus
Rh raphe nucleus
S spinal cord
SAC stratum album centrale
SC suprachiasmatic nucleus
SFGS stratum fibrosum et griseum superficiale
SGC stratum griseum centrale
SGN secondary gustatory nucleus
sgt secondary gustatory tract
SM stratum marginale
SO secondary octaval nucleus
SPV stratum periventriculare
SR superior reticular formation
T tangential nucleus
TGN tertiary gustatory nucleus
TL torus longitudinalis
TLA torus lateralis
TP posterior tubercle
tpm pretectomammillary tract
TS torus semicircularis
TSvl torus semicircularis, ventrolateral nucleus

TSc	torus semicircularis, central nucleus
V	ventral telencephalon (subpallium)
VIN	abducens nucleus
VIIs	sensory root of VII
VC	cerebellar valvula
Vd	dorsal nucleus of ventral telencephalon
vgt	ventral glycinergic tract
VH	ventral horn of spinal cord
VL	rostroventral part of the TSC glycinergic neuropil
Vl	lateral nucleus of ventral telencephalon
VM	ventromedial nucleus of thalamus
Vp	postcommissural nucleus of ventral telencephalon
Vs	supracommissural nucleus of ventral telencephalon
vTg	GLYT2-positive ventral tegmental nucleus
Vv	ventral nucleus of ventral telencephalon
X	vagal nerve
Xm	vagal motor nucleus
zl	zona limitans intrathalamica

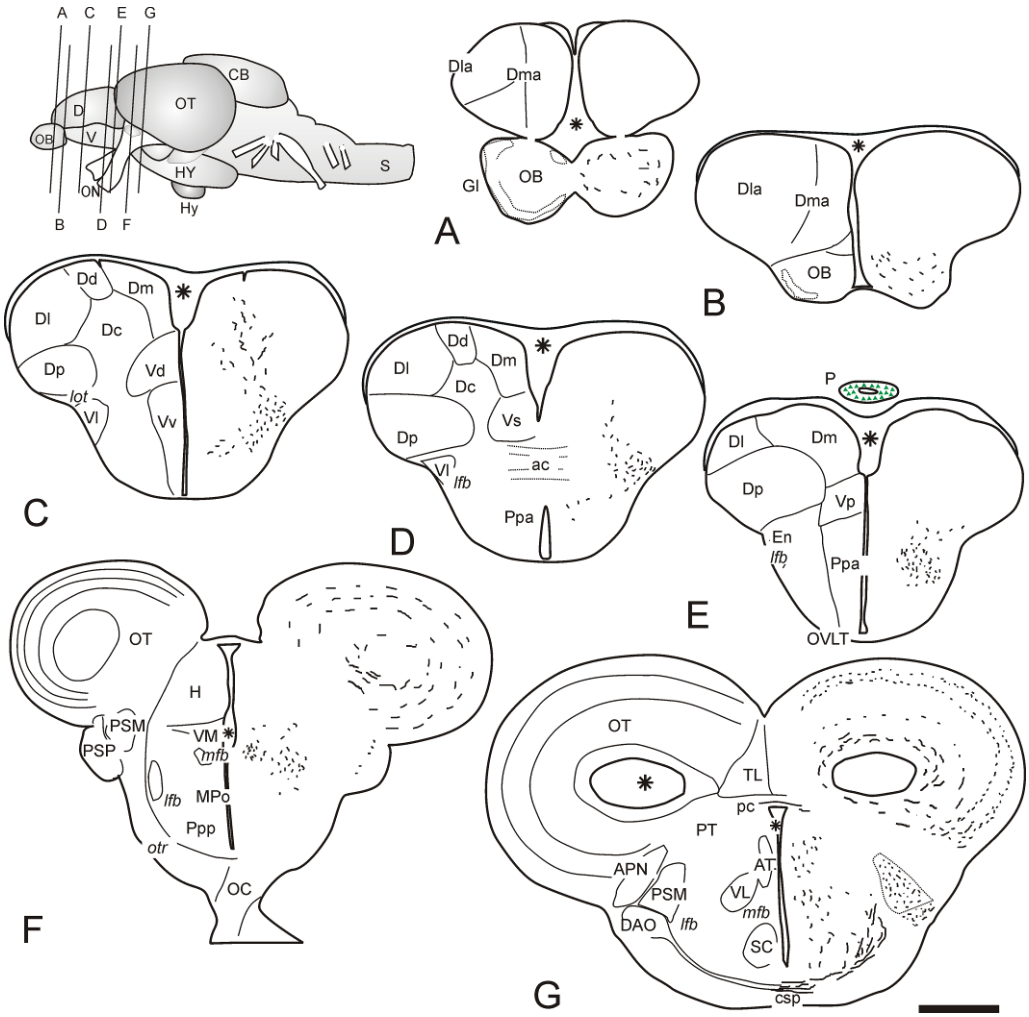

Figure 1. Schematic drawings of transverse sections of the adult Tg(*glyt2:gfp*) zebrafish brain showing the main anatomical structures in the left side. The distribution of populations showing GFP-positive/GLYT2-positive perikarya (large black dots), GLYT2-positive/GFP-negative (lozenges, in pink in the online version) and GFP-positive-GLYT2-negative neurons (triangles, in green in the online version) is shown in the right side of sections. GFP-positive fibers (dashes) are also represented in the right side. In levels J-L, the periventricular cell layer of the torus semicircularis is represented by the gray-shaded region on the left side. The schematic profiles of the three characteristic pairs of glycinergic reticulospinal neurons and their descending axons are also drawn on the left side of levels P-X (in red in the online version). The GFP-negative Mauthner cell is drawn on the left in level O and the Mauthner axon (arising from the contralateral MC) is also indicated in levels P-X (in blue in the online version). In the cerebellar crest (levels O-R), some GFP-positive crest cell

dendrites are depicted. The levels of sections are indicated by lines in the figures representing a lateral view of the brain. Asterisks indicate ventricular cavities. For abbreviations, see list. Scale bars: 200 µm.

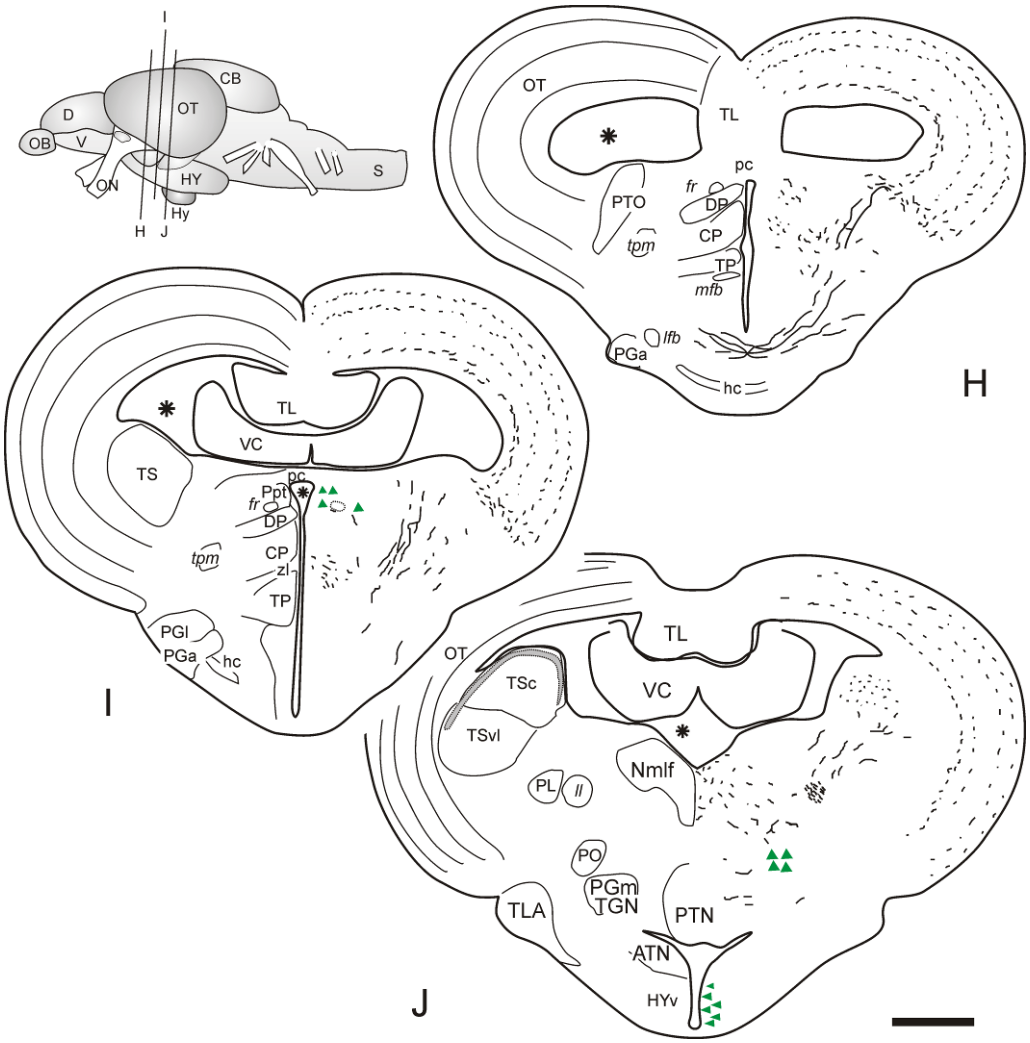

Figure 1-continuation

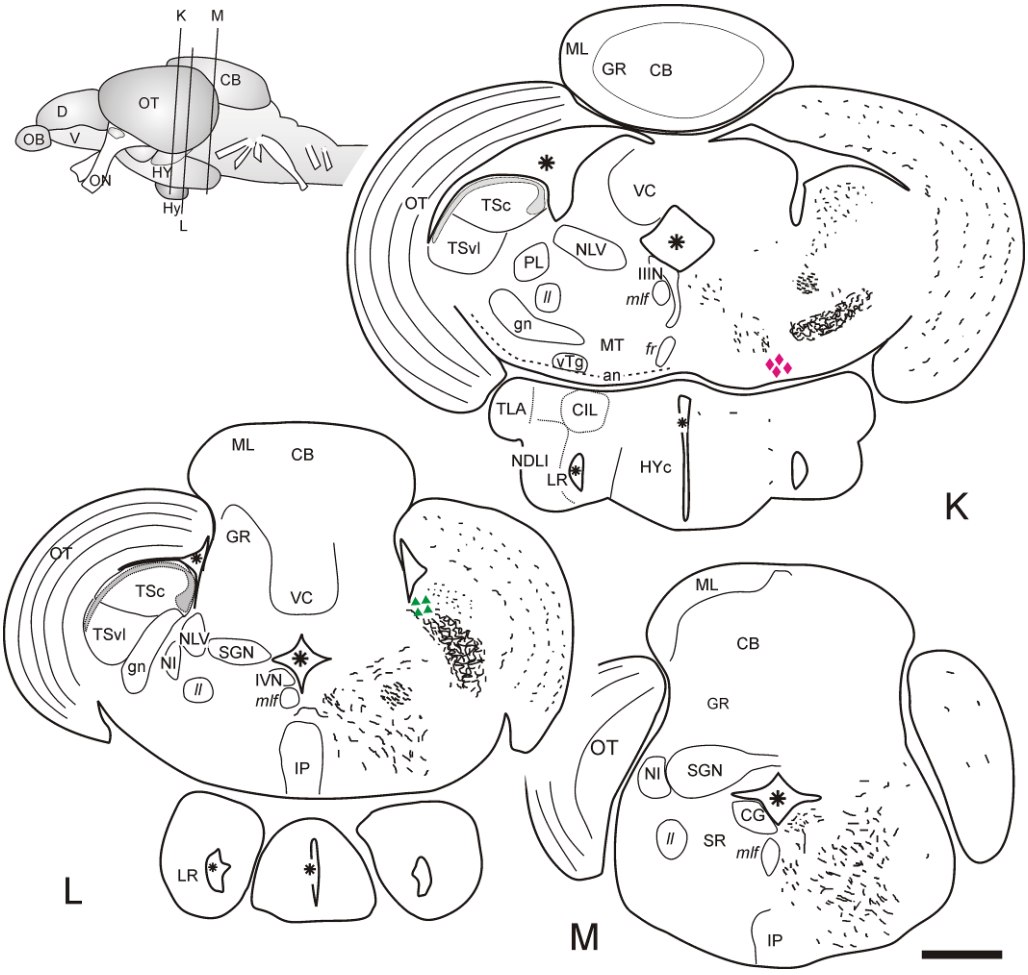

Figure 1- continuation

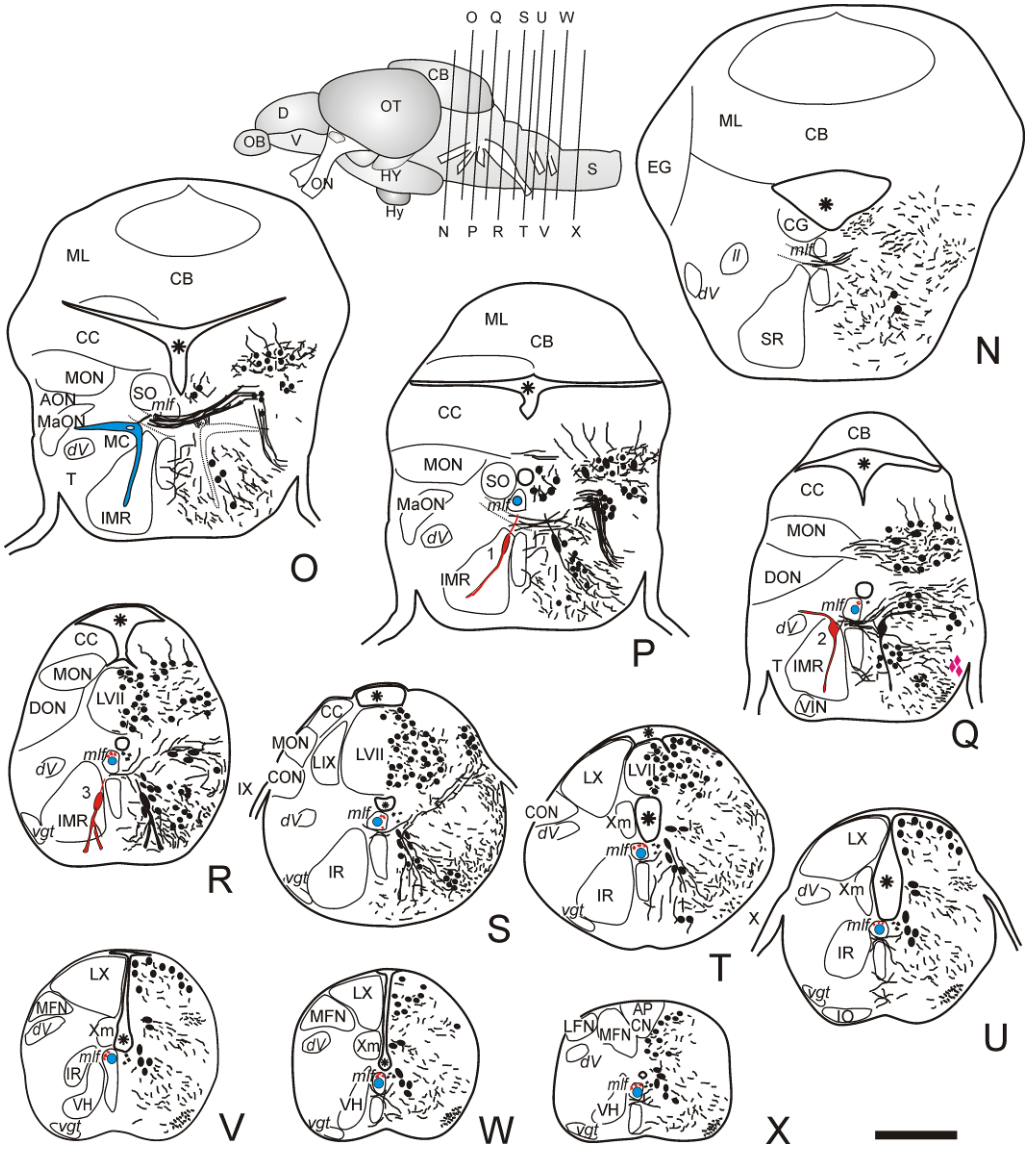

Figure 1- continuation

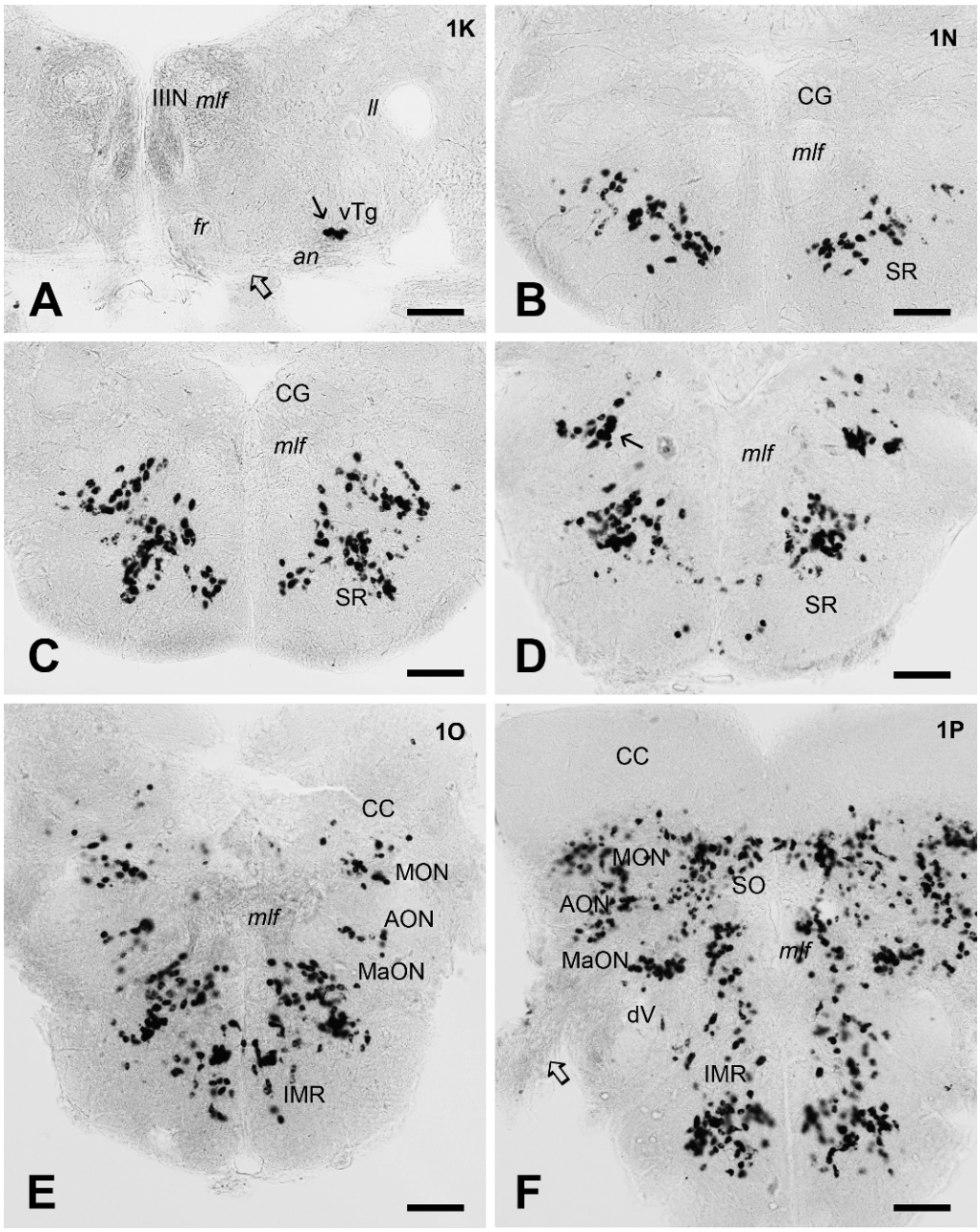

Figure 2. Photomicrographs of representative sections of the zebrafish brain showing perikarya expressing GLYT2 mRNA, ordered from rostral (A) to caudal (J). **A**, GLYT2-positive neurons are observed in a small group of the midbrain tegmentum (black arrow). **B-J**, Numerous GLYT2-positive cells were distributed throughout most regions of the rhombencephalon. Note the large differences in staining intensity among neuronal populations. For abbreviations, see list. Black arrow in D points to the dorsal cell cluster caudal to the dorsal trigeminal motor nucleus. Outlined arrows in A and F indicate the oculomotor and octaval nerve, respectively. Approximate correspondence with

levels in drawings of Figure 1 is indicated in the upper right corner. Scale bars = 100 μm.

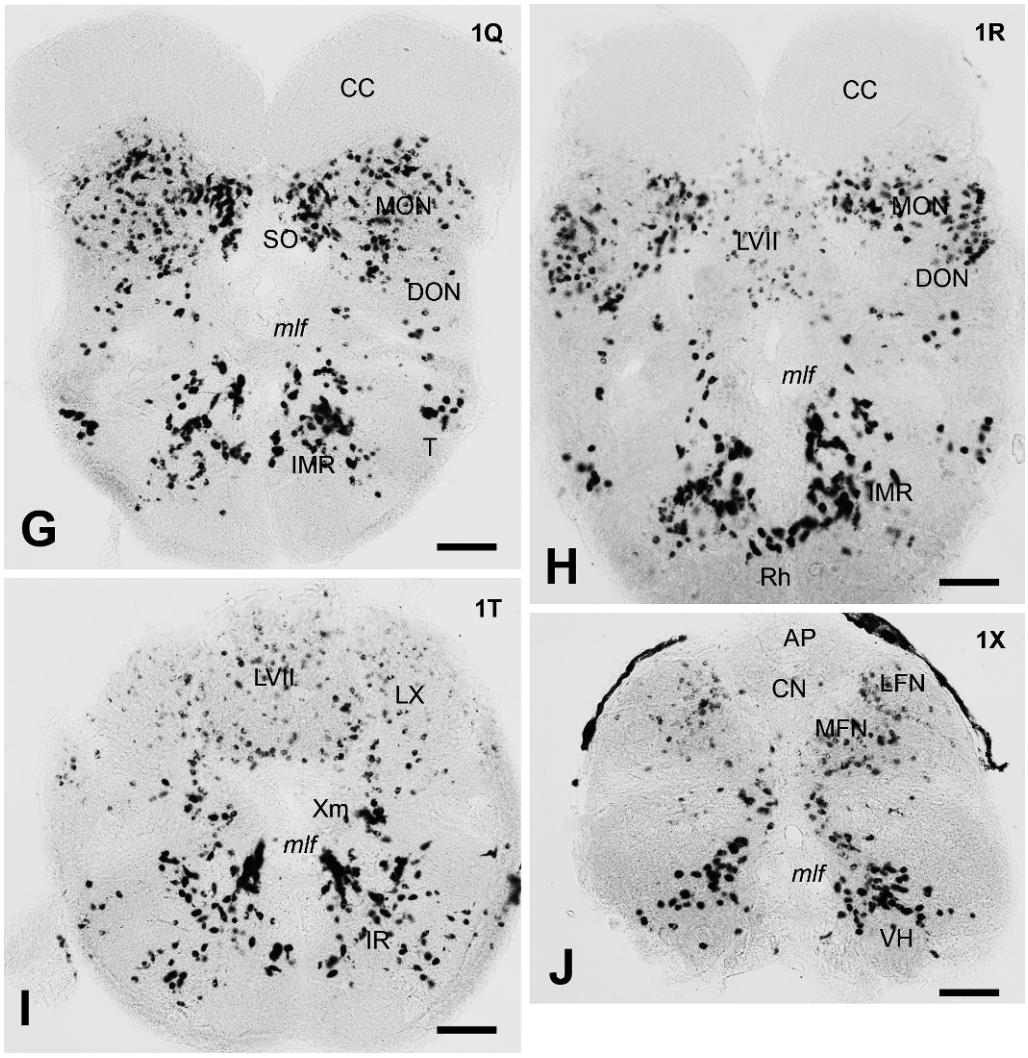

Figure 2- continuation

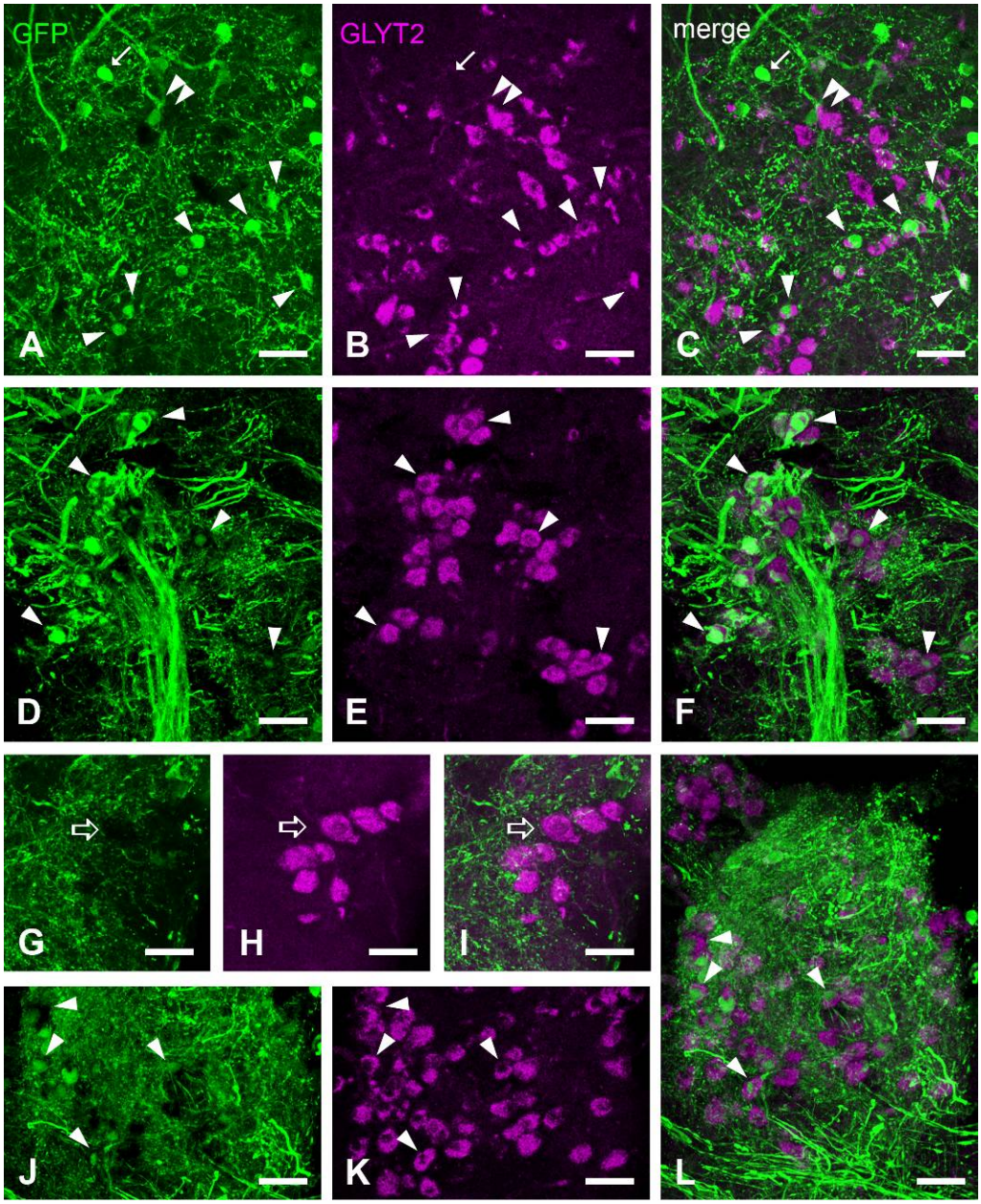

Figure 3. Confocal photomicrographs of representative populations of the octavolateral region showing partial colocalization of GFP-immunofluorescence (green channel, left) and GLYT2 mRNA *in situ* hybridization (magenta channel, central) in the right panels (merged channels). **A-C**, Medial octavolateral nucleus showing two types of positive neurons. Small cells (arrowheads) show clear colocalization but strong GLYT2 reaction in crest cells (double arowhead) obscured GFP immunofluorescence, although it is visible in the apical dendrite of the pointed cell. Note also GFP-positive/GLYT2 negative cells (arrow). **D-F**, Glycinergic nucleus at the level of the magnocellular octaval nucleus showing GLYT2/GFP double labeled

cells (arrowheads). **G-I**, Tangential nucleus exhibiting GLYT2-positive but GFP-negative cells (outlined arrow). **J-L**, Secondary octaval nucleus exhibiting double positive neurons, some indicated by arrowheads. Scale bars: 20 µm.

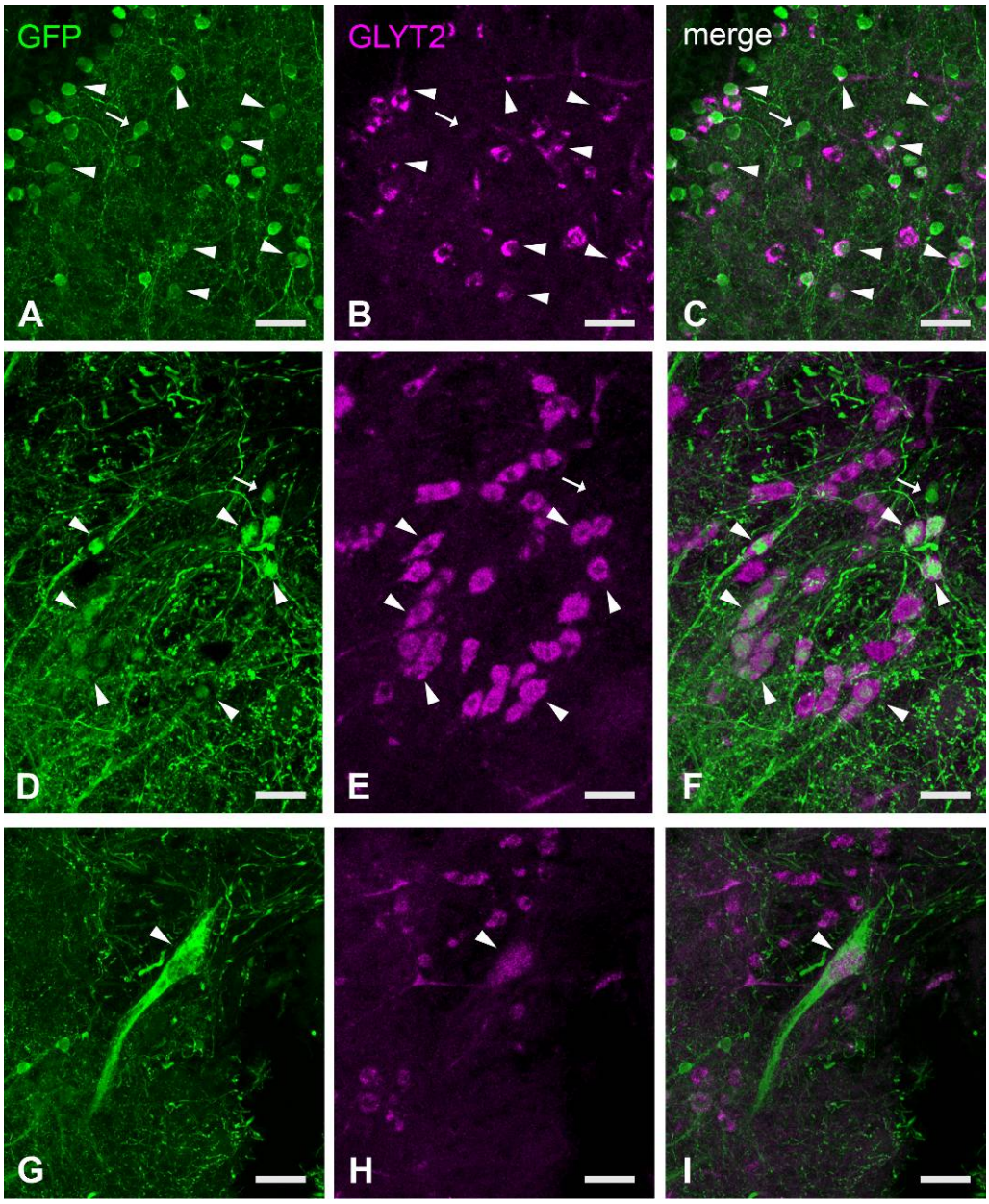

Figure 4. Confocal photomicrographs of representative rhombencephalic glycinergic populations showing partial colocalization of GFP-immunofluorescence (green channel, left) and GLYT2 mRNA *in situ* hybridization product (magenta channel, central) in the right panels (merged channels). **A-C**, Section of the facial lobe showing faint GLYT2 staining in a part of the GFP-positive cells (arrowheads). Note also GFP-positive/GLYT2 negative cells (arrow). **D-F**, Section of the intermediate reticular formation. Arrowheads point to some cells showing clearly GFP /GLYT2 colocalization, the arrow to a GFP-positive/GLYT2-negative cell. **G-I**, Large GFP-positive

reticular cell (arrowhead) showing moderate GLYT2 expression. This cell corresponds to the spinal-projecting glycinergic cells shown in figure 11F. Scale bars: 20 µm.

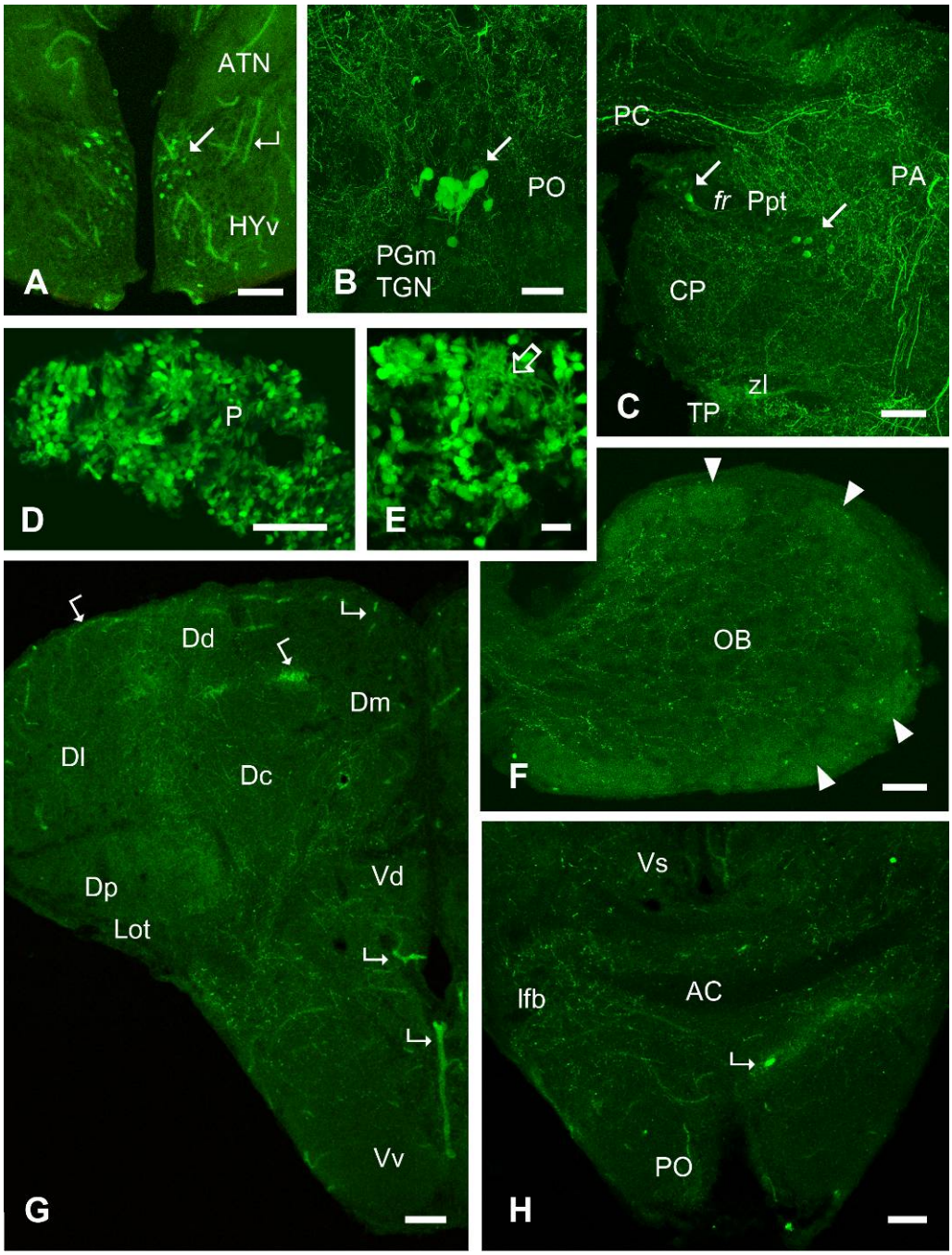

Figure 5. Sections of the adult Tg(*glyt2:gfp*) zebrafish forebrain showing GFP-expressing cells (A-E), and GFP expression in fibers of the olfactory bulb (F) and telencephalon (G-H). **A**, Transverse section of the ventral hypothalamus showing a group of small cells (arrow) below the anterior tuberal nucleus. **B**, Transverse section of the diencephalon passing through the medial preglomerular nucleus showing a group of medium-sized GFP-positive cells (arrow). **C**, Transverse section of the caudal diencephalon showing scattered

small GFP-positive cells lateral to the posterior commissure (arrows). Note also a band of GFP-positive fibers in the zona limitans and ascending fibers densely innervating the pretectal area. **D-E**, Sagittal section passing through the pineal organ showing the large population of small GFP-positive cells. In E, note processes of these cells coursing to a basal neuropil in the neuroepithelium (outlined arrow). **F**, Sagittal section showing GFP-positive fibers scattered through the olfactory bulb, mainly in inner regions. Arrowheads point to olfactory glomeruli. Rostral is at the right. **G**, Transverse section showing the scarcity of GFP-positive fibers in the dorsal telencephalic area (pallium). **H**, Transverse section at the level of the anterior commissure showing GFP-positive fibers coursing mostly laterally to it. Angled arrows in A, G and H point to autofluorescent blood vessels. A,D-H, GFP fluorescence; B-C, GFP immunofluorescence. For abbreviations, see list. Scale bars: 50 µm (A-D, F-H), 10 µm (E).

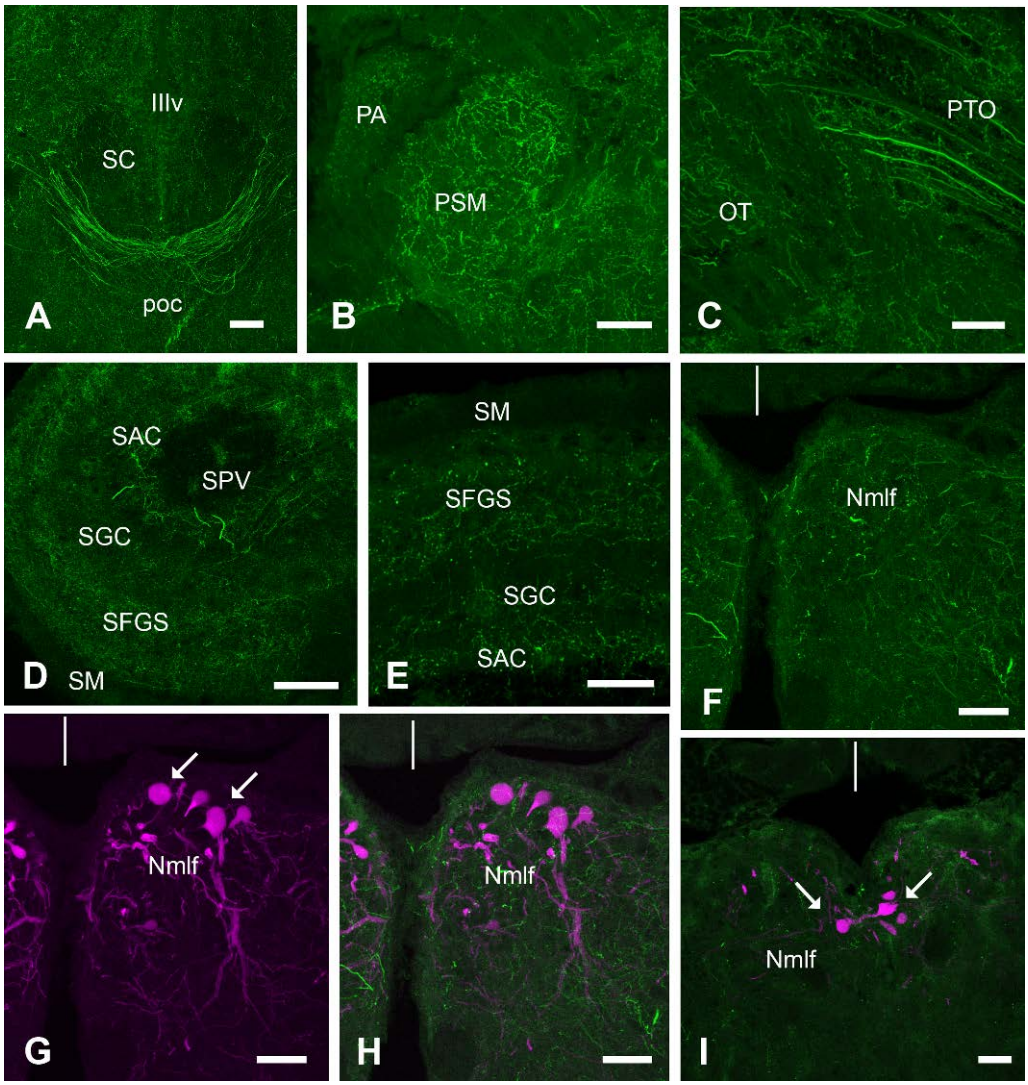

Figure 6. Confocal photomicrographs of transverse sections through the diencephalon and optic tectum of the adult Tg(*glyt2:gfp*) zebrafish. **A**, Section at the level of the suprachiasmatic nucleus showing the crossing of GFP-positive fibers in the postoptic commissure. **B**, Section though the superficial pretectum showing the rich GFP-positive innervation of the magnocellular nucleus. **C**, Section at a lateral level of the pretoral region showing the entrance of thick GFP-positive fibers to the optic tectum. **D**, Section through the rostral optic tectum showing thick GFP-positive fibers in the stratum album centrale and thinner fibers in other strata. **E**, Detail of plexuses of GFP-positive fibers in the layers of the optic tectum. **F-H**, Photomicrographs of the nucleus of the medial longitudinal fascicle showing in F the GFP-positive fibers (green), in G the large cells retrogradely labeled from the spinal cord (in magenta) and in H the merged channels. **I**, Section passing through the rostral midbrain

tegmentum showing scarce GFP-positive fibers in the red nucleus, which shows cells retrogradely labeled from the spinal cord (arrowed, in color in the digital edition). For abbreviations, see list. A, GFP immunofluorescence; B-I, GFP fluorescence (alone or combined with biocytin detection). In B, C, D and E, medial is at the right; in F-I, the midline is indicated by vertical dashes. Scale bars: 50 µm (A-C, E-I), 100 µm (D).

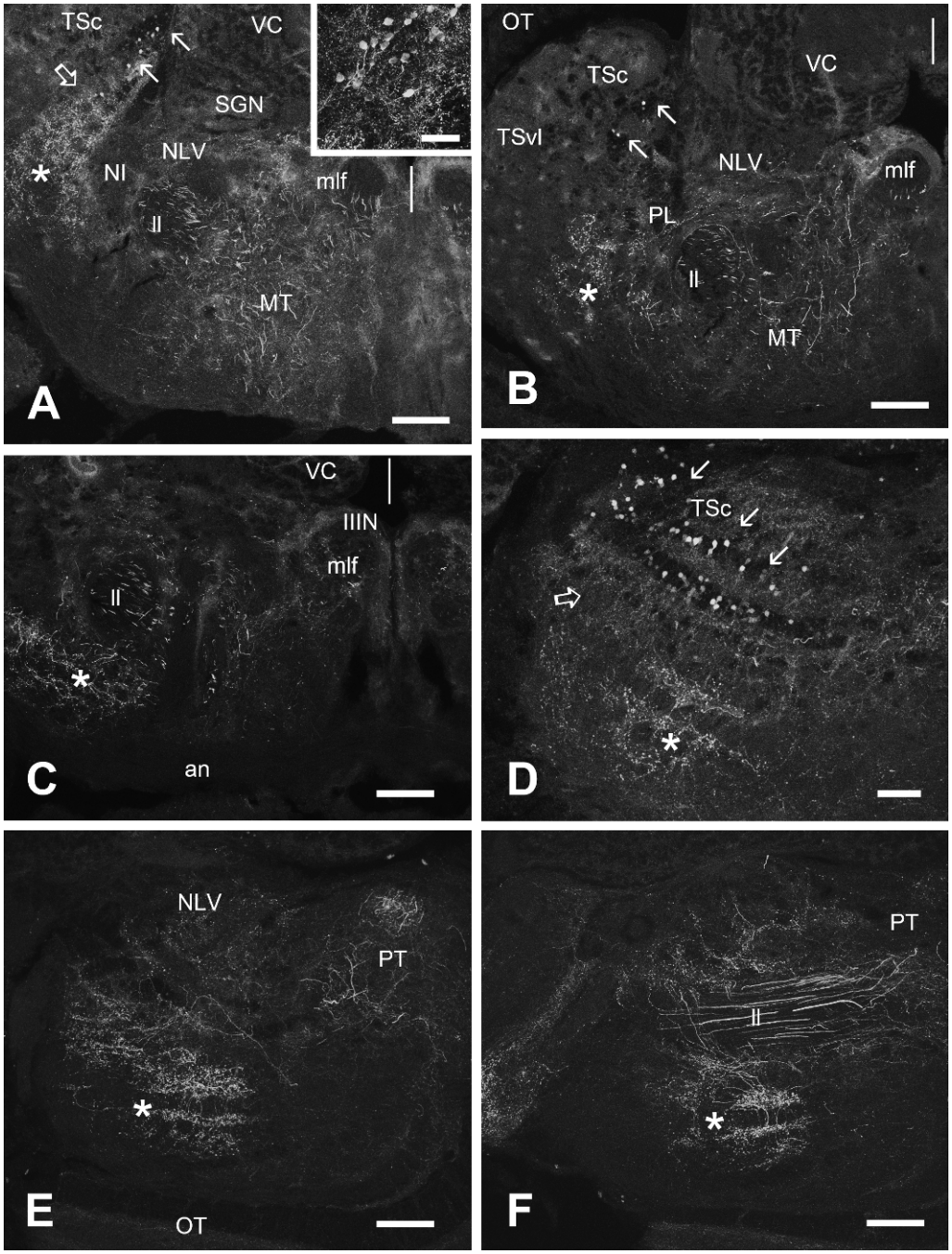

Figure 7. Confocal photomicrographs of transverse (A-C) and parasagittal (D-F) sections through the mesencephalic tegmentum of the adult Tg(*glyt2:gfp*) zebrafish showing the distribution of GFP-expressing cells and fibers. **A** and **D**, Sections at the level of the medial fiber plexus of the torus semicircularis/midbrain lateral reticular region (outlined arrows and asterisks, respectively) and the GFP-expressing small cells located in the medial region of the central nucleus of the torus (arrows). Inset in A, detail of the cells. **B-C** and **E-F**, Sections showing the dense plexus of glycinergic fibers in the

midbrain lateral reticular region (asterisks). Note also thick glycinergic fibers ascending in the lateral longitudinal fascicle toward the pretectum and tectum. In A-C, midline is indicated by vertical dashes. In D-F, rostral is at the right. For abbreviations, see list. All figures are of GFP fluorescence except the inset in figure A, which was revealed by GFP immunofluorescence. For the anatomical location of the GFP-positive cell containing region in Nissl-stained sections, see Figure 8. Scale bars: 100 µm (A-C, E-F), 50 µm (D), 25 µm (inset in A).

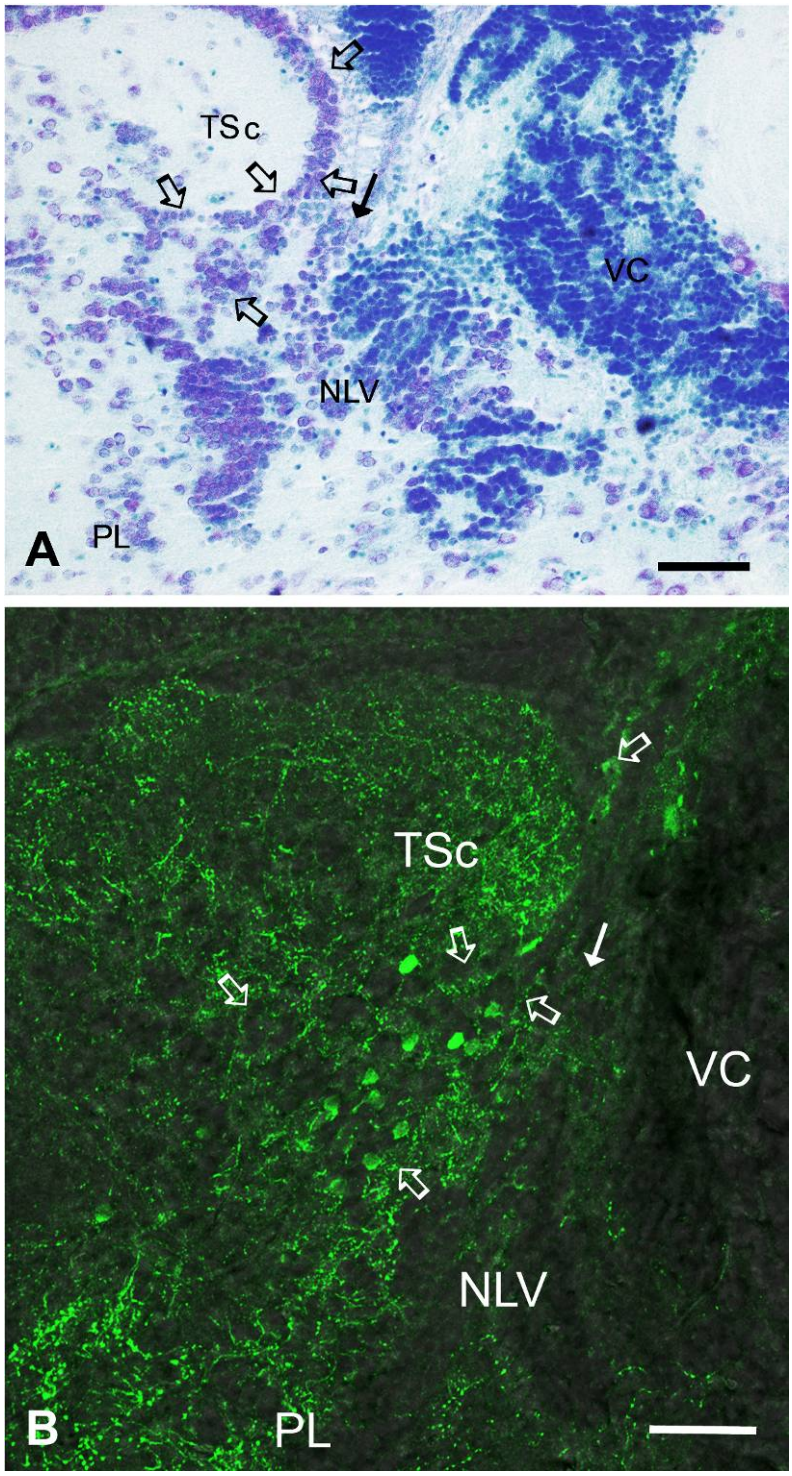

Figure 8. Nissl-staining (A) and GFP fluorescence (B) in transverse sections of adult zebrafish passing through the region of the central nucleus of the torus semicircularis showing the location of the region containing GFP-positive cells with respect to the TSc periventricular layer and other nuclei and structures. Thick outlined arrows indicate the same region in both sections (Figure in color in the online version). The thin arrows point to the ventricular

sulcus separating the torus and the lateral nucleus of the valvula. A, light microscopy, wild type zebrafish. B, confocal fluorescence and background microscopy, transgenic zebrafish. For abbreviations, see list. Scale bars, 50 µm.

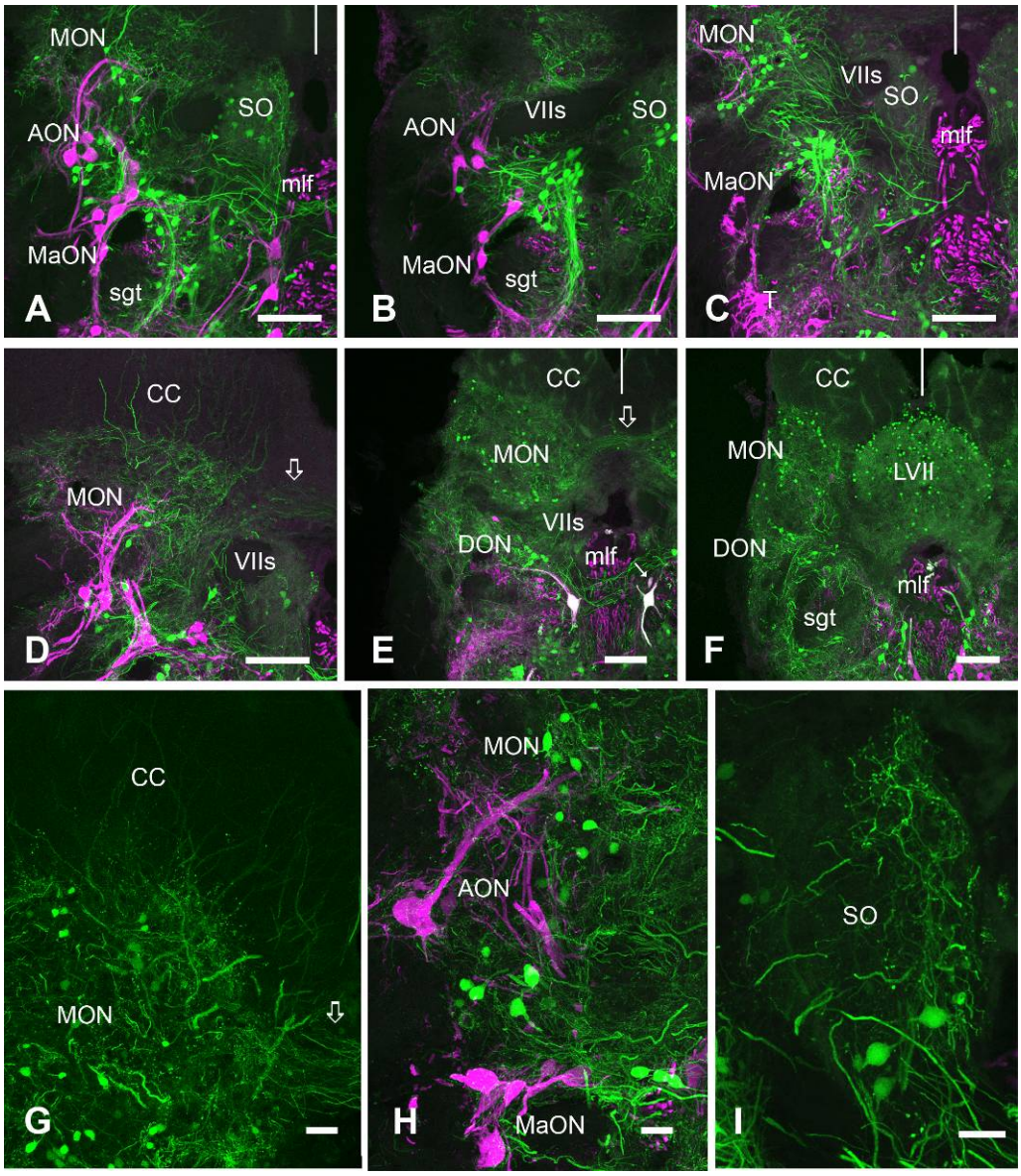

Figure 9. **A-F**, Confocal photomicrographs of transverse sections through the octavolateral region of adult Tg(*glyt2:gfp*) zebrafish showing the distribution of GFP-positive neurons (green) and their topographical relationship to spinal projecting neurons of this region (in magenta). In E, small arrow points to a small spinal-projecting cell. **G**, Detail of GFP-positive crest cells of the medial octavolateral nucleus sending long dendrites to the cerebellar crest. Note also

small glycinergic cells in this nucleus. **H**, Detail of GFP-positive cells in the octavolateral nuclei (MON, AON and MaON) at the level of the octaval nerve entrance. Retrogradely labeled octaval cells are shown in magenta. **I**, Detail of the large GPF-positive neurons of the secondary octaval nucleus and the rich terminal field. Outlined arrows in D-E and G point to GFP-positive fibers crossing in a dorsal commissure joining secondarily the octavolateral nuclei of both sides. In A, C, E, F, midline is indicated by vertical dashes. In other panels, medial is at the right. For abbreviations see list. Scale bars: 100 µm (A-F), 50 µm (D), 25 µm (H, I).

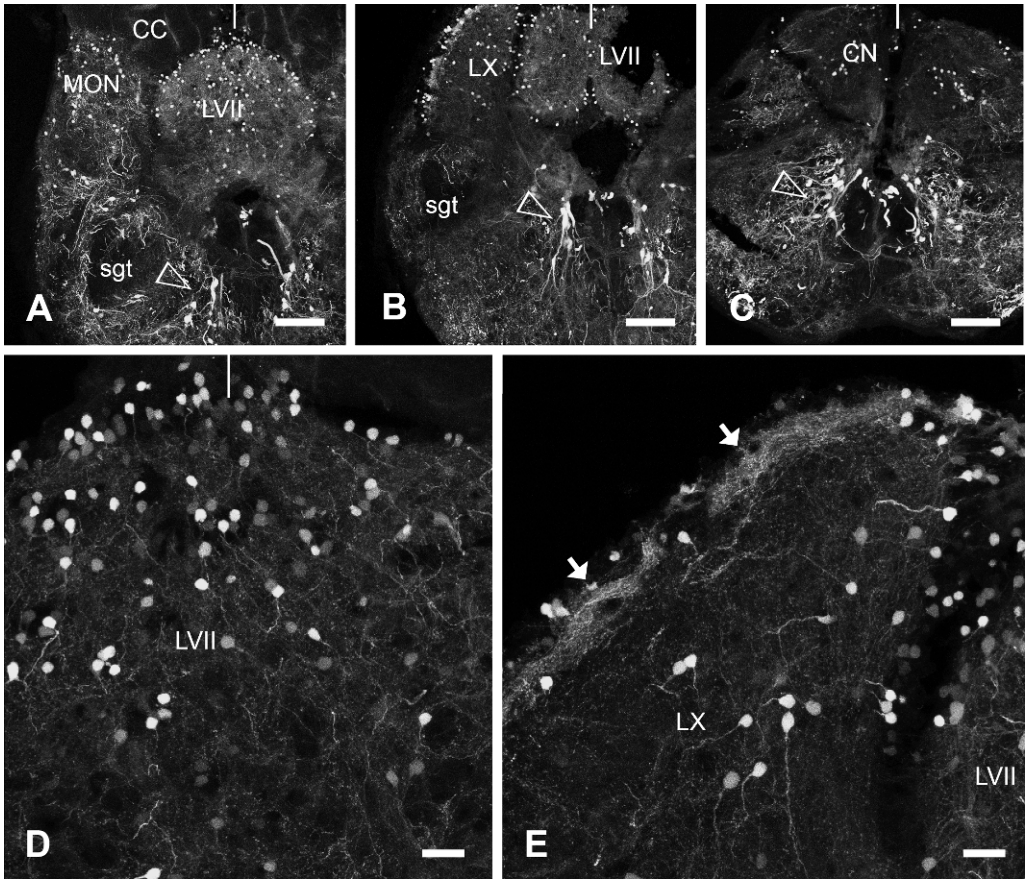

Figure 10. **A-C**, Confocal photomicrographs showing the distribution of GFP-expressing neurons in transverse sections of the medulla of adult Tg(*glyt2:gfp*) zebrafish at the level of the facial lobe (A), vagal lobe (B) and commissural nucleus (C). Outlined arrowheads point to glycinergic reticular neurons. **D**, Detail showing the appearance of small glycinergic neurons of the facial lobe. **E**, Detail showing the neurons of the vagal lobe and the superficial layer of glycinergic fibers (arrows). In A-D, vertical dashes indicate the midline. For abbreviations, see list. Scale bars: 100 µm (A-C), 20 µm (D-E).

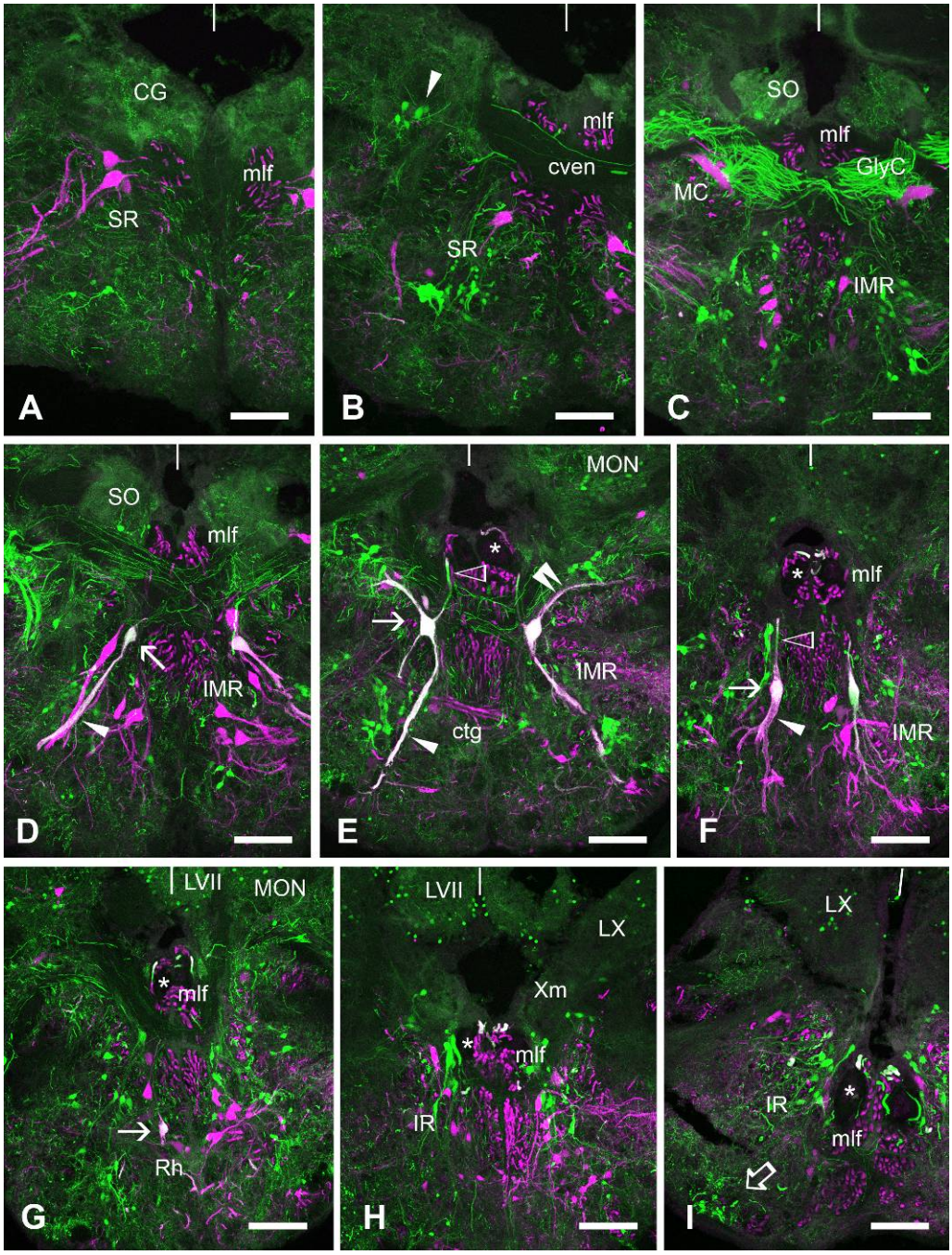

Figure 11. Confocal photomicrographs of transverse sections through the rhombencephalon of the adult Tg(*glyt2:gfp*) zebrafish arranged rostrocaudally showing GFP-expressing structures in green, and cells and fibers labeled from the spinal cord in magenta. Double-labeled cells appear in white. **A**-**B**, Sections showing the most rostral rhombencephalic glycinergic cells located ventrally to the large reticulospinal neurons of the superior reticular nucleus. A small dorsal cluster of GFP-positive neurons (arrowhead) is shown caudally to the dorsal trigeminal motor nucleus (not appearing at this level). **C**, Section at the level of

the Mauthner cells showing abundant glycinergic neurons in the intermediate reticular nucleus. Note the conspicuous GFP-positive commissural fibers at the level of Mauthner cells. **D**, Section showing the rostral pair of GFP-positive reticulospinal neurons (arrow) located caudally to the Mauthner cell (photomontage of two adjacent sections). Note the ventrolateral dendrite (arrowhead). **E**, Section showing the second pair of glycinergic reticulospinal neurons (arrow). These cells with contralateral axons correspond to the accessory Mauthner cell. Note long dorsal (double arrowhead) and ventral (arrowhead) dendrites of these cells and the exit of axons (outlined arrowhead). Angled arrow points to a double-labeled small cell close to a large glycinergic reticulospinal cell. Photomontage of three adjacent sections. **F**, Section at a level just rostral to the facial lobe showing the third pair of large reticulospinal glycinergic neurons (arrow). Note the thick branched ventral dendrite (arrowhead) and the initial segment of the axon (outlined arrowhead). **G-I**, Sections showing GFP-positive neurons in the inferior reticular nucleus at the level of the facial lobe (G-H) and vagal lobe (I). In G, note a retrogradely labeled glycinergic neuron in the raphe nucleus (arrow). Asterisks in E-I indicate the Mauthner axon. In E-I, note also thick axons of retrogradely labeled GFP-positive cells in the dorsal part of the medial longitudinal fascicle. Outlined arrow in I points to a conspicuous ventrolateral fascicle of glycinergic fibers coursing in the caudal medulla and spinal cord. Vertical dashes indicate the midline. For abbreviations, see list. Scale bars: 100 µm (A-I).

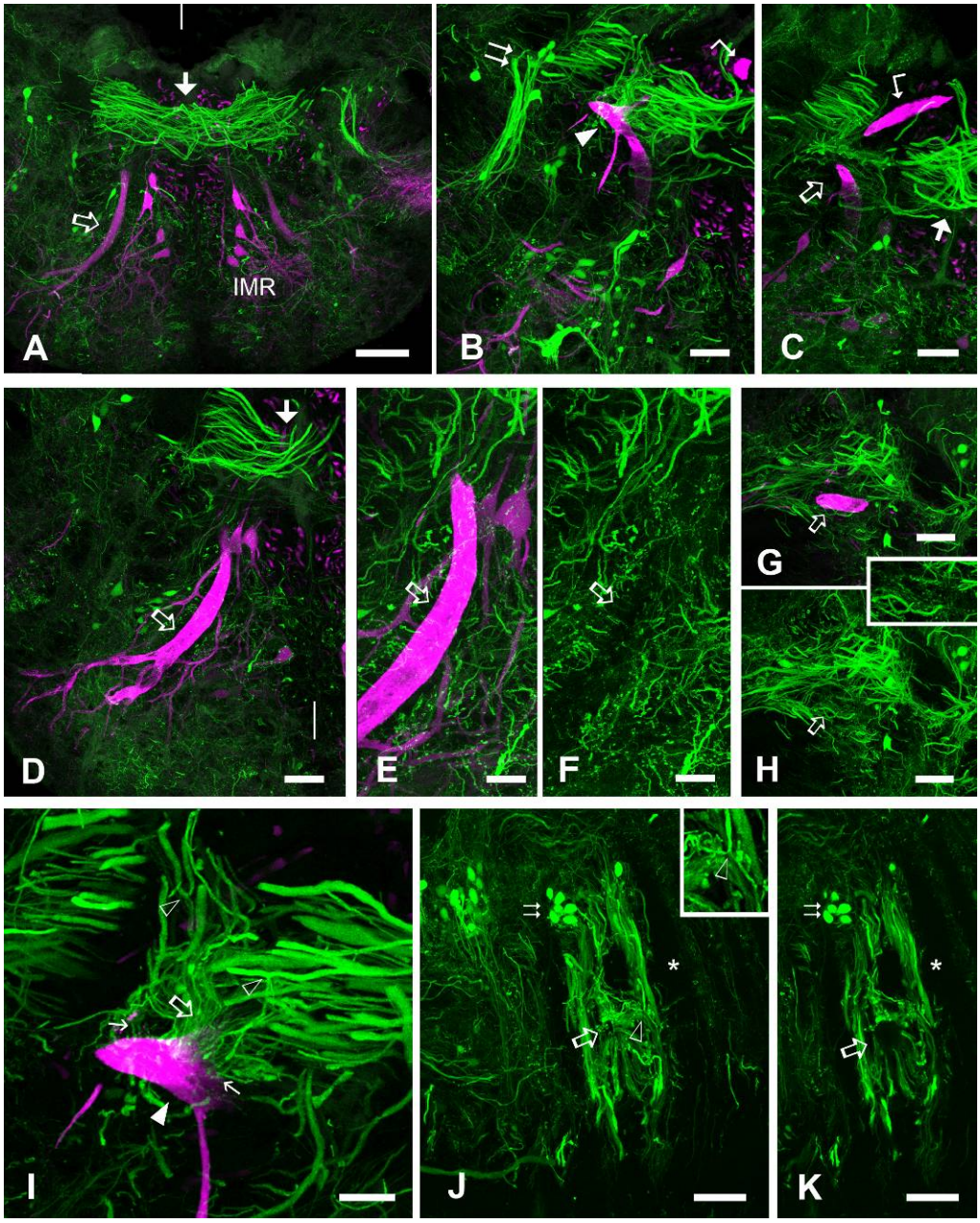

Figure 12. Confocal photomicrographs of transverse (A-G) and oblique sagittal sections of the rhombencephalon of adult Tg(*glyt2:gfp*) zebrafish showing the glycinergic innervation of the Mauthner cell (MC). Glycinergic structures appear in green and retrogradely labeled cells in magenta. **A**, Section passing through the commissure of thick glycinergic fibers (thick arrow) at the level of retrogradely labeled Mauthner neurons. The outlined arrow points to the ventral dendrite of MC. **B**, Section passing through the labeled MC cell body (arrowhead) at the level of the axon exit, which is surrounded by numerous glycinergic fibers. Note also the compact group of glycinergic cells (double

arrow) laterally to MC and the Mauthner axon (angled arrow). **C**, Section passing through the MC axon (angled arrow). The outlined arrow points to the ventral dendrite and the thick arrow points to the commissural fibers. **D**, Section showing the branching of the ventral dendrite (outlined arrow) of a retrogradely labeled MC. The white arrow points to glycinergic commissural fibers. **E-F**, Detail of the thick ventral MC dendrite (outlined arrow) showing scarce glycinergic innervation. E, merged channels, E', glycinergic fibers. **G-H**, Detail of the thick ventral dendrite (outlined arrow) showing rather scarce glycinergic innervation. F, merged channels, F', glycinergic fibers. Inset, detail of the small glycinergic boutons around the MC dendrite. **I**, Transverse section at the level of the dorsal glycinergic commissure showing numerous thin collaterals of thick fibers that contact the region of the MC perikaryon (white arrowhead) around the axon hillock indicated by thin white arrows. Outlined arrowheads indicate branching fibers. The outlined thick arrow points to the axon cap. **J, K**, Details of two confocal planes of a sagittal section passing through the axon cap (indicated by the outlined arrow) of the MC (unlabeled) at proximal (J) and more distal (K) levels showing thin collaterals of the thick commissural glycinergic fibers embracing the axon hillock region. Double arrows point to glycinergic neurons, the asterisk indicates a glycine-negative dorsal commissural tract. Inset in J shows a detail of the branching of the glycinergic fiber pointed by an arrowhead. In A and D, vertical dashes indicate the midline. In B-C and E-I, medial is at the right. In J-K, rostral is at the right. For abbreviation, see list. Scale bars: 100 µm (A), 50 µm (B, C, D, G-H, J, K), 30 µm (inset in H), 25 µm (E-F, I, inset in J).

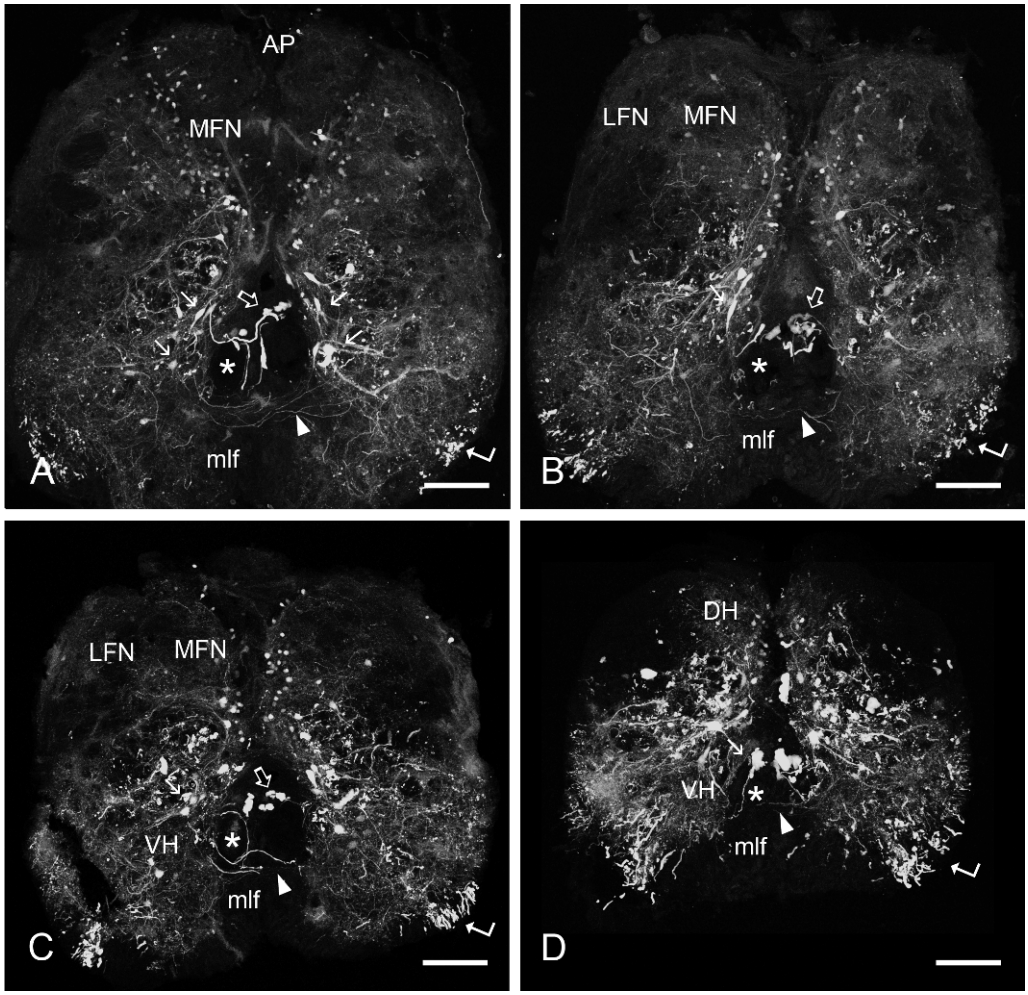

Figure 13. **A-D**, Transverse sections through the caudal medulla and rostral spinal cord from more rostral (A) to more caudal (D) showing the distribution of GFP-positive cells and fibers in adult Tg(*glyt2:gfp*) zebrafish. Note the different cells size of dorsal and ventral horn cells, and the abundance of glycinergic processes in the ventral horn and ventrolateral funiculus. Thin arrows point to ventral horn medium-sized glycinergic neurons. Outlined arrows point to thick glycinergic axons coursing in the dorsal part of the mlf. Arrowheads point to commissural fibers crossing between the dorsal and ventral parts of the mlf. Asterisks indicate the location of MC giant axons. Angled arrows point to a ventrolateral tract of thick glycinergic axons. For abbreviations, see list. Scale bars: 100 µm (A, B, C, D).

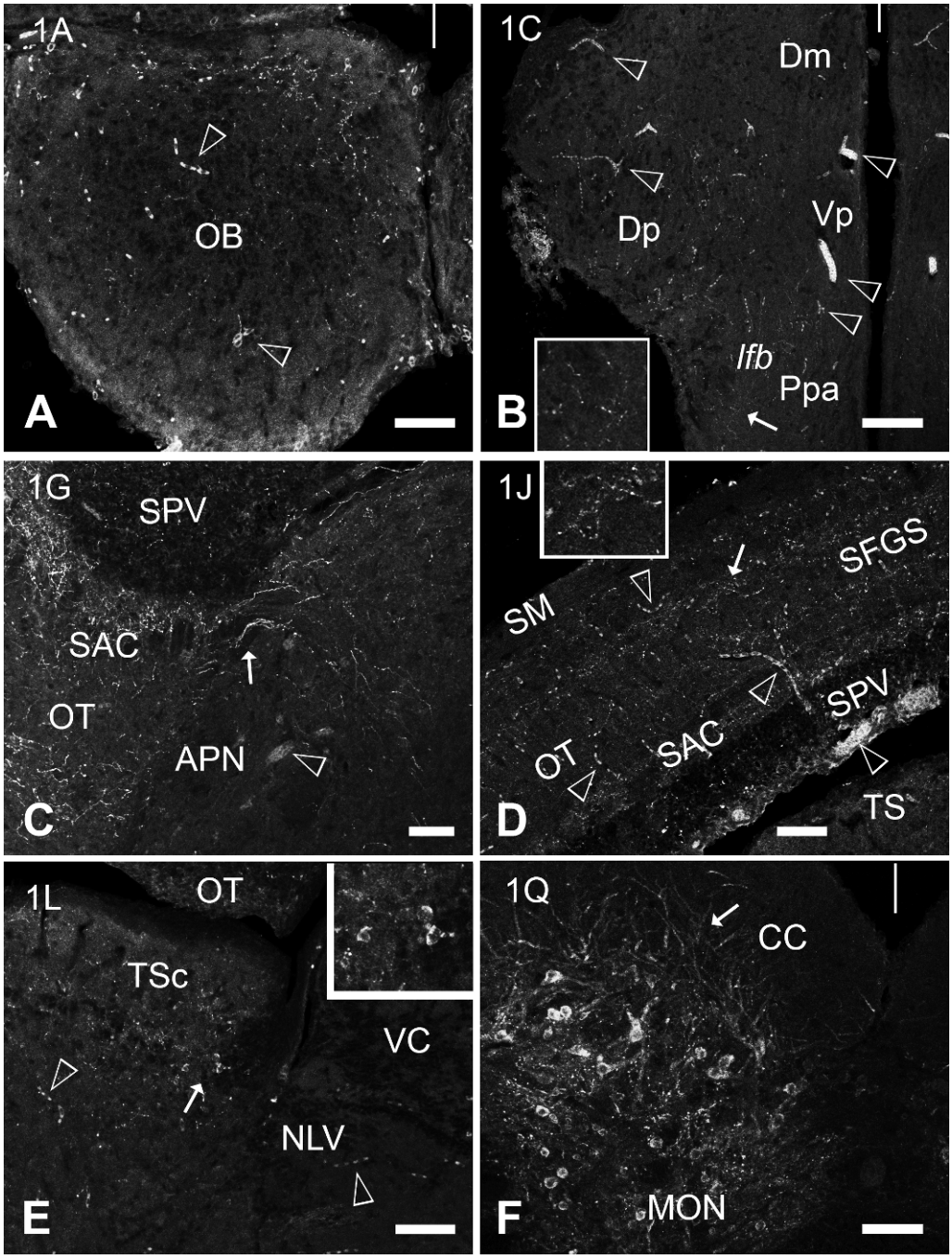

Figure 14. Confocal photomicrographs of transverse sections of adult wild type zebrafish brain showing glycine immunofluorescence in neurons (in E-F) and fibers. **A**, Section showing glycine-ir fibers in the olfactory bulb. Outlined arrowheads point to blood vessels. **B**, Section of the caudal telencephalon showing scarce glycine-ir fibers. The arrow points to fibers shown in the inset. Outlined arrowheads, blood vessels. **C**, Transition between the pretectum and rostral optic tectum showing glycine-ir fibers passing to the tectum (arrow). Outlined arrowhead, blood vessel. **D**, Optic tectum showing the stratified

distribution of glycine-ir fibers. The arrow points to fibers shown in the inset. Outlined arrowheads, blood vessels. **E**, Torus semicircularis at the level of the small-celled glycinergic population (arrow). Inset, detail of these glycine-ir cells. Outlined arrowheads, blood vessels. **F**, Medial octavolateral nucleus showing larger cells with dendrites extending in the cerebellar crest (arrow) and small cells. Vertical bars indicate the midline (A, B, F). In C, D and E, medial is at the right. For abbreviations, see list. Correspondence with levels in Figure 1 is indicated. Magnification of insets is double than in corresponding figures. Scale bars, 50 µm (A, C, D, E, F), 100 µm (B).

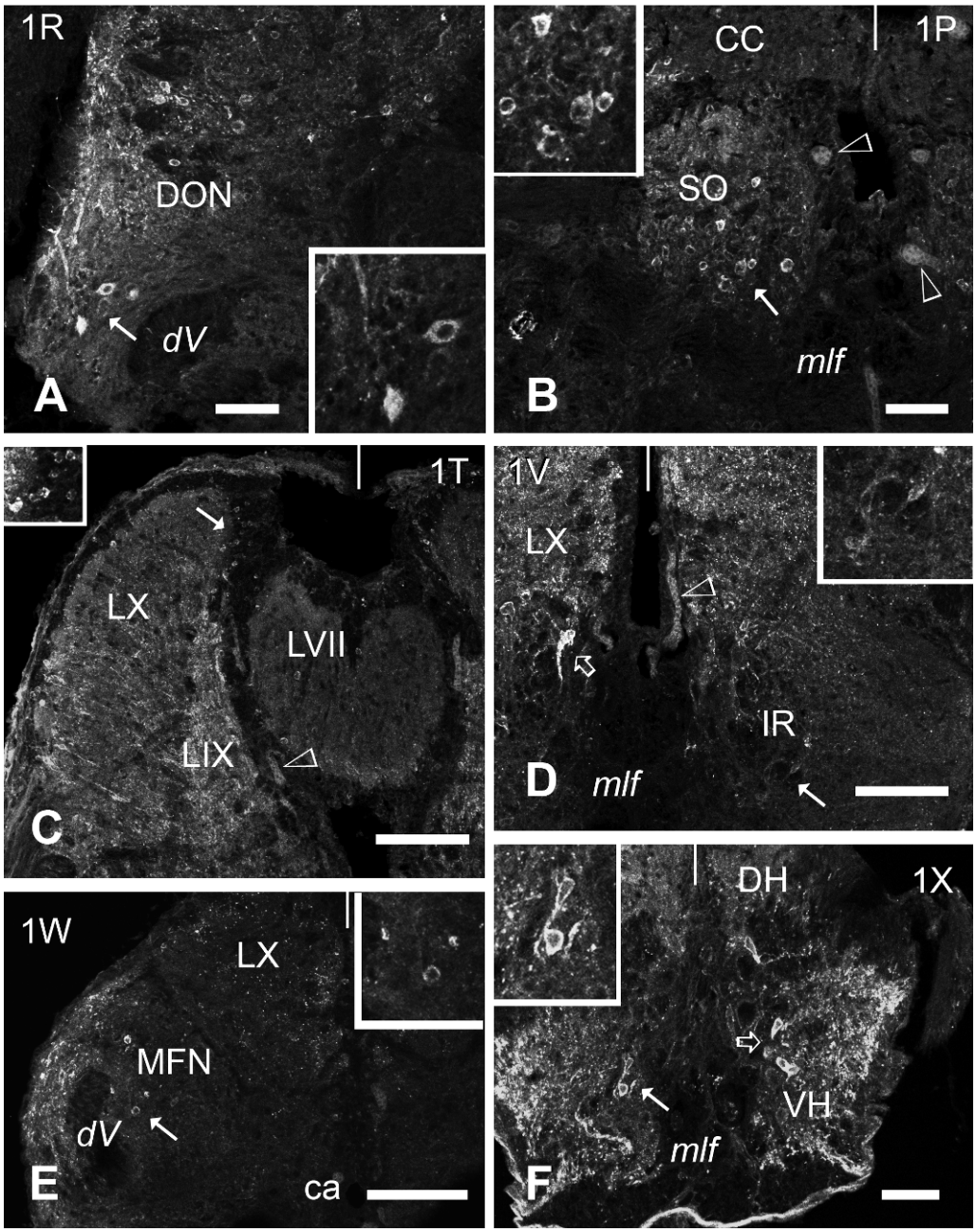

Figure 15. Confocal photomicrographs of transverse sections of adult wild type zebrafish brain showing glycine immunofluorescence in neurons and fibers. **A**, Alar rhombencephalon showing glycine-ir cells in the descending octaval nucleus and lateral to the trigeminal descending tract (arrow). Inset, detail of arrowed cells. **B**, Secondary octaval nucleus showing glycine-ir neurons (arrow). Inset, detail of arrowed cells. Outlined arrowhead, blood vessel. **C**, Section through the facial and vagal lobes showing small glycine-ir cells. Inset, detail of the arrowed cells. Outlined arrowhead, blood vessel. **D**, Section showing glycine-ir cells in the inferior reticular formation. The arrowed small

cells are magnified in the inset. The outlined arrow points to a larger reticular neuron. Outlined arrowhead, blood vessel. **E**, Section through the caudal medulla showing glycine-ir cells in the medial funicular nucleus (arrow). Inset, detail of arrowed cells. **F**, Section of the spinal cord showing glycine-ir cells of the ventral horn (arrows). Inset, detail of the solid arrow-pointed cells. Vertical bars indicate the midline (A-F). For abbreviations, see list. Correspondence with levels in Figure 1 is indicated. Magnification of insets is double than in corresponding figures. Scale bars, 50 µm (A, B, F), 100 µm (C, D, E).